batteries

MDPI

Review

AI-Enabled Battery Storage and Electric Vehicle Flexibility for Power-Quality-Constrained Photovoltaic Integration: A Critical Review

Amr S. Zalhaf [1], Hongzhi Jiang [2], Yang Han [2], Mohamed Mohandes [1,3], Ali Al-Shaikhi [1,3], Abdelaziz M. Gebril [4] and Suliman Aladhadh [5,*]

[1] IRC for Sustainable Energy Systems (IRC-SES), King Fahd University of Petroleum and Minerals, Dhahran 31261, Saudi Arabia mohandes@kfupm.edu.sa (M.M.); shaikhi@kfupm.edu.sa (A.A.-S.)
[2] School of Mechanical and Electrical Engineering, University of Electronic Science and Technology of China, Chengdu 611731, China
[3] Electrical Engineering Department, King Fahd University of Petroleum and Minerals, Dhahran 31261, Saudi Arabia
[4] Electrical Power and Machines Engineering Department, Faculty of Engineering, Tanta University, Tanta 31511, Egypt
[5] Department of Information Technology, College of Computer, Qassim University, Buraydah 51452, Saudi Arabia
* Correspondence: s.aladhadh@qu.edu.sa

Abstract

High photovoltaic (PV) penetration in distribution networks can be limited by voltage rise, unbalance, harmonics, thermal loading, and converter-current constraints before the available solar resource is fully utilized. Battery energy storage systems (BESS) and electric vehicle (EV) flexibility can relieve some of these limits, but their contribution depends on battery state, degradation, converter headroom, mobility, communications, and point of common coupling requirements. This critical review asks when artificial intelligence (AI) improves the use of stationary and mobile battery flexibility under those constraints. The synthesis compares these engineering dimensions qualitatively and includes a source-level comparison of 30 selected sources, together with focused comparisons of battery technologies and AI constraint-enforcement methods. Across the reviewed evidence, fast reactive and waveform-support services are often constrained by converter current more directly than by battery energy, whereas energy shifting and vehicle-to-grid operation are strongly affected by state of charge, availability, efficiency, and aging. AI is most defensible as a forecasting, estimation, and supervisory layer; it does not replace electrical feasibility or battery safety limits. Usable PV energy, meaning energy delivered after curtailment, conversion losses, and battery constraints, is not the same quantity as a larger nominal hosting-capacity rating. The review therefore recommends reporting net recovered PV energy together with compliance margin, converter utilization, battery throughput, aging assumptions, uncertainty, fallback behavior, and validation maturity.

Keywords: artificial intelligence; battery energy storage systems; electric vehicles; vehicle-to-grid; photovoltaic integration; power quality; battery degradation; hosting capacity; distribution networks

Check for updates

Academic Editor: King Jet Tseng

Received: 18 September 2026
Revised: 17 October 2026
Accepted: 21 October 2026
Published: 2 November 2026

Copyright: © 2026 by the authors. Licensee MDPI, Basel, Switzerland. This article is an open access article distributed under the terms and conditions of the Creative Commons Attribution (CC BY) license.

1. Introduction

Distribution systems are becoming active renewable-generation platforms rather than passive delivery networks. In photovoltaic (PV)-rich feeders, the practically relevant quan-

tity is not installed PV nameplate capacity alone but the portion of available solar power that can be exported or locally consumed without violating voltage, thermal, unbalance, harmonic, protection, or converter constraints. Classical hosting-capacity studies established that feeder topology, impedance, and voltage-control design make distributed-generation penetration strongly location-dependent [1,2]; later work showed that harmonic distortion, background waveform distortion, and frequency-dependent network impedance can also become binding constraints [3–5]. These mechanisms connect power quality (PQ) directly to renewable-energy utilization because each binding constraint can translate into curtailment, additional storage cycling, flexible-demand rescheduling, or network reinforcement.

Battery energy storage systems (BESS) and electric vehicles (EVs) make the PV operating boundary time-dependent. Stationary BESS can absorb excess solar energy, discharge later, and provide fast active or reactive support, while controllable EV charging and vehicle-to-grid (V2G) operation can align demand with midday PV production, alter feeder peaks, and contribute converter-based voltage support [6–10]. The electrical capability of these resources is not equivalent to continuously available flexibility, because state of charge (SOC), state of health (SOH), battery temperature, degradation, converter current, round-trip losses, charger connection, departure-energy requirements, communication availability, and user participation all restrict the service that can be delivered.

Artificial intelligence (AI) can improve forecasts, battery-state estimates, and sequential dispatch under uncertainty. Its outputs remain subordinate to converter ratings, feeder limits, SOC/SOH bounds, protection, and fallback control. Battery-management reviews document progress in learning and digital twins [11]; recent studies extend learning to battery–grid coordination and physically constrained charging [12,13]. The question is whether these methods improve usable PV energy under the same physical and lifetime constraints as conventional control.

The central research question is whether stationary and mobile batteries increase *usable PV energy* after the applicable point-of-common-coupling (PCC), feeder, converter, battery, mobility, and deployment constraints are enforced. Four subsidiary questions make that comparison explicit: (i) which electrical or PQ mechanisms become binding as PV penetration increases; (ii) which BESS or EV services can relax each mechanism, and at what cost in battery duty and converter headroom; (iii) when AI-enabled forecasting, estimation, or control add value over deterministic alternatives under the same physical constraints; and (iv) what validation evidence is required before a reported gain can be transferred from simulation to deployment. This distinction matters because a strategy that raises installed hosting capacity while increasing annual curtailment, conversion loss, cycling, or battery wear may deliver less renewable energy than a smaller nominal hosting increase evaluated over representative operating conditions.

Existing reviews cover EV-related voltage, harmonic, and loading effects [14–16]; PV–storage architectures, voltage regulation, and energy management [17–20]; and broad AI-enabled grid-storage applications [21,22]. Table 1 compares their organizing questions with the present synthesis. Here, reported gains are compared through the disturbance, actuator, battery duty, compliance boundary, and validation level. Battery-aging and V2G evidence [23,24] constrains the transferable claim: a larger hosting rating does not establish greater PV delivery after losses, cycling, and electrical limits are accounted for.

Filip et al. quantify the effect of EV/BESS deployment on LV PV hosting [25], while Khunkitti et al. optimize BESS/PV placement and capacity in an EV-integrated feeder [26]. These studies establish the combined system boundary. The present review examines how concurrent PQ limits, battery condition, conversion losses, and validation affect interpretation of such gains. Usable PV energy is the system outcome; battery energy, current capability, SOC/SOH, temperature, degradation, and availability determine the flexibility that can support it.

Table 1. Scope of the present review relative to recent reviews. The final column identifies what each review does not treat as a primary organising variable; it does not assert that the topic is absent.

Reference	Primary Focus	Key Complementary Strength	Not Treated as a Primary Organising Variable
[14]	EV charging, grid interaction, PQ, and stability	Detailed treatment of charger-related electrical effects and mitigation	PV-energy utilization and stationary battery duty are not the main organizing outcomes
[15]	Voltage regulation in low-voltage networks with renewables and EVs	Strong voltage-regulation and coordinated-control perspective	Harmonic, thermal, battery-lifetime, and multi-timescale storage constraints require joint treatment
[16]	Broad EV impacts and mitigation in distribution networks	Broad EV integration and operational coverage	Renewable-energy utilization and battery-service cost are not the primary synthesis variables
[17]	PV–energy-storage voltage regulation	Direct PV/BESS voltage-control coverage	EV availability, V2G, harmonic constraints, and deployment evidence lie outside the principal boundary
[18]	Hybrid energy storage integrated with renewable generation	Battery-focused review of hybrid energy storage system (HESS) configurations, control, optimization, applications, and PQ-related renewable-integration motivations	Does not center PV–EV/V2G–BESS distribution feeders, simultaneous PCC constraints, usable PV energy, or deployment-evidence maturity
[19]	PV–battery grid-forming configurations and coordinated control	Direct treatment of PV/BESS architecture and grid-forming control	EV/V2G availability, multi-PQ constraints, usable PV energy, and deployment maturity are outside its principal review boundary
[20]	BESS optimization in buildings and energy communities	Battery-focused synthesis of applications, optimization, SOC, and degradation	Distribution-feeder PQ, PCC harmonic constraints, EV mobility, and PV hosting are not the main synthesis axes
[21]	AI-driven optimization of grid-scale BESS	Systematic treatment of AI methods, techno-economic performance, environmental effects, and policy/regulatory issues for grid-scale storage	Does not center distribution-feeder PCC constraints, EV/V2G availability, simultaneous PQ mechanisms, or usable PV energy as the principal outcome
[22]	Artificial intelligence (AI)-enabled BESS for renewable energy	Broad synthesis of machine learning (ML), deep learning, reinforcement learning (RL), battery management, degradation, PV/wind, microgrids, and smart grids	The synthesis narrows AI to PQ-constrained usable-PV recovery with stationary/mobile battery flexibility, hard feasibility, and validation boundaries
[11]	AI and digital twins for lithium-ion battery management	Detailed SOC/SOH/remaining useful life (RUL), lifecycle, cloud–edge, and intelligent battery management system (BMS) synthesis	Does not organize the evidence around PCC power-quality limits, EV/V2G availability, and usable PV energy in distribution feeders
[23]	V2G applications and battery cycle aging	Direct battery-lifetime perspective for mobile grid storage	Does not jointly organize stationary BESS, PV curtailment, multi-PQ constraints, and validation maturity
[24]	Rechargeable batteries for grid-scale energy storage	Broad 2026 assessment of battery technologies, performance, safety, and grid applications	Distribution-feeder PQ, EV flexibility, and usable PV energy are not the central system-level synthesis axis

The review evaluates BESS and EV technologies by their effects on PV hosting, curtailment, compliance margin, net usable solar energy, battery throughput, and lifecycle limitations. A reported improvement in voltage, harmonics, cost, or hosting is therefore

interpreted only after the feeder boundary, regulated quantity, converter headroom, battery duty, vehicle availability, control assumptions, and validation platform are identified. The four subsidiary questions stated above provide the structure for Sections 3–6, so the discussion moves from the physical constraint to the available flexibility, then to control and validation rather than presenting technologies as independent catalogues.

Table 2 compares selected system studies, battery experiments, and reviews used in the synthesis. The entries illustrate distinct engineering claims and validation boundaries; they are not a representative sample of the bibliography.

Table 2. Selected sources informing the critical synthesis.

Source	System and Objective	Battery and Control Representation	Validation Level	Reported Findings and Scope Limitations
[25]	Low-voltage (LV) distribution network; effect of EV and BESS deployment on PV hosting	Stationary and mobile storage flexibility in a feeder-level hosting study	System-level numerical study	Establishes that EV/BESS deployment changes PV hosting; does not by itself provide a cross-study accounting of PQ mechanisms, battery aging, and net delivered PV energy.
[26]	EV-integrated distribution feeder; coordinated BESS/PV placement and sizing	Optimization of location and capacity	Optimization/feeder simulation	Establishes that placement and sizing materially affect the combined PV–EV–BESS boundary; transfer depends on feeder model, objectives, and battery assumptions.
[20]	Buildings and energy communities; BESS optimization and grid services	SOC- and degradation-aware storage optimization	Review synthesis	Provides a strong battery-operation and degradation perspective; distribution-feeder PQ and PCC harmonic constraints are outside its main comparison boundary.
[21]	Grid-scale BESS; AI-enabled techno-economic and environmental optimization	Broad AI-method and grid-storage synthesis	Systematic review	Establishes the breadth of intelligent grid-storage optimization; it does not use distribution-feeder PQ constraints or usable PV energy as its principal comparison outcome.
[22]	Renewable-energy BESS applications across PV, wind, microgrids, and smart grids	ML, deep learning, RL, battery management, and degradation	Comprehensive review	Establishes a broad 2026 AI–BESS taxonomy. The present review therefore does not claim novelty from AI coverage itself; its narrower contribution is the PQ-constrained energy-accounting and validation boundary.
[27]	Distribution-network Volt–Var control	Model-augmented reinforcement learning with a safety layer	Feeder simulation	Illustrates constraint correction of learned dispatch; battery lifetime and full PCC compliance are not demonstrated.
[28]	V2G cycling using real-world usage profiles	Cell-level lifetime response to V2G duty	Experimental battery study	Supplies direct evidence that V2G duty and cycling assumptions matter for lifetime claims; feeder-support value still depends on charger availability and network constraints.
[29]	PV charge allocation in multi-battery energy systems	Physics-informed neural-network control	Intelligent-control study	Supports physically constrained battery allocation; it is battery/control evidence rather than direct proof of distribution-feeder PQ compliance.

Table 2. *Cont.*

Source	System and Objective	Battery and Control Representation	Validation Level	Reported Findings and Scope Limitations
[30]	PV–wind laboratory microgrid with battery–supercapacitor storage	Hybrid storage transient buffering	Laboratory experiment	Demonstrates experimental transient-buffering behavior and links storage dynamics to AC-side performance; laboratory scale does not by itself establish utility deployment maturity.
[31]	MW-class zinc–iron flow battery source–grid–load–storage coordination	SOC estimation and coordinated power allocation	Large-system model	Extends the evidence beyond lithium-ion systems and shows the importance of internal battery state; chemistry, service objectives, and feeder context limit direct transfer to PV-rich LV networks.

2. Review Scope and Analytical Framework

This narrative critical review synthesizes sources selected for their engineering relevance to PQ-constrained PV integration with stationary and mobile batteries. Heterogeneous feeder models, battery duties, compliance boundaries, and validation methods preclude a statistical meta-analysis or a universal ranking of controllers. The bibliography is an expert-selected evidence base; it is not the included-study cohort of a systematic review.

2.1. Source Selection and Scope

Sources were selected for their contribution to one of four questions: the electrical mechanism limiting PV utilization, the battery or EV service available to relieve it, the control constraints governing that service, and the evidence supporting transfer to operation. Selection considered methodological detail, relevance to the distribution/PCC boundary, and the distinction between modeled, laboratory, and field outcomes. Standards and original project reports were used for compliance definitions and deployment evidence; battery experiments were used for aging and ripple claims. Reviews supplied context rather than independent validation of a controller.

The evidence base includes foundational studies predating 2015 and targeted recent publications beyond June 2026. These sources are retained when they establish a physical mechanism, measurement definition, experimental battery response, or directly relevant system comparison. Publication dates therefore do not follow the narrower window of the supplementary OpenAlex check. Historical database query logs were not retained, so the cited literature cannot be assigned a retrospective database-specific screening flow. IEEE Xplore, Scopus, Web of Science, and ScienceDirect are consequently not reported as a reproducibly searched database set. Pure materials studies without a grid-interface implication and unrelated applications are outside the review scope.

2.2. Source Appraisal and Supplementary Coverage Check

Supplementary Tables S1 and S5 record the system boundary, reported outcome, validation level, and limits of use of selected sources discussed in the main comparisons. These purposive assessments support interpretation of specific claims; their proportions do not estimate the validation distribution of the literature. Supplementary Table S3 profiles the references actually cited in the current manuscript.

An independent OpenAlex coverage check was executed on 2 October 2026 using eleven title-field queries. The archived API requests retrieved publications dated 1 January 2015–16 September 2026; the reported comparison subset retains records dated through 30 June 2026.

This publication cutoff is distinct from the execution date. A rule-based Python 3.13.13 script applied metadata filters and keyword expressions to available titles and abstracts, assigning one primary classification code per record. It classified the 10,487 records remaining after metadata triage automatically; they were not independently assessed by human reviewers. The terms, rules, stage counts, and record-level outputs are supplied in Supplementary Table S4.

The narrow title queries and automated rules provide a supplementary check of topical coverage, not the selection process for the bibliography. Their small overlap with cited sources cannot establish completeness or representativeness, and an automated pass is not full-text eligibility or inclusion. The coverage-check counts are therefore kept in the supplement and are not used to infer how many studies support the review's conclusions. Selected-source appraisal and the illustrative comparisons remain separate from this automated register.

2.3. Analytical Synthesis Framework and Evidence Hierarchy

Table 3 defines the dimensions used for qualitative comparison. Table 4 applies them to ten illustrative sources, recording the binding constraint, battery or EV duty, validation, and outcome used in this review. The source assessments in Supplementary Tables S1 and S5 provide further claim-specific detail.

Table 3. Analytical dimensions used for qualitative evidence synthesis.

Dimension	Extracted Attributes	Engineering Significance for Renewable Integration	Representative Anchors
System and PCC boundary	Voltage level, phases, grid strength, location, and monitoring point	Device-level improvement does not establish feeder hosting; impedance and phase coupling govern transfer	[1,2,4]
Binding PQ constraint	Disturbance, metric, bandwidth, and assessment interval	The binding mechanism determines whether P/Q control, phase balancing, filtering, storage, or reinforcement is relevant	[3,5,32,33]
Battery duty	Power, SOC/SOH, temperature, throughput, ripple, and reserve	Energy shifting changes throughput; fast support also depends on converter headroom and DC-side buffering	[6,28,34,35]
EV availability	Connection, bidirectionality, departure energy, SOC, and compensation	Charger capability and user constraints determine whether scheduled flexibility is actually available	[7,8,23,36,37]
Control architecture	Local, centralized, or distributed control; update horizon	Comparisons require matched resource limits and adequate measurement/communication speed	[38–42]
AI/data-driven role	Forecasting, state estimation, scheduling, and action correction	Prediction/reward gains require a demonstrated effect on feasible dispatch, PV delivery, or battery duty	[11–13,43]

Table 3. *Cont.*

Dimension	Extracted Attributes	Engineering Significance for Renewable Integration	Representative Anchors
Converter and resource limits	P/Q/current envelope, harmonics, thermal derating, efficiency, and shared reserves	Nominal ratings overstate flexibility when concurrent services share current and energy headroom	[40,44–47]
Validation maturity	Simulation, real-time test, laboratory, pilot, or field operation	Planning feasibility, fast dynamics, interoperability, and operational readiness need different evidence	[3,48–50]
Compliance basis	Applicable document, point, metric, and aggregation method	Equipment emissions, installation allocation, and supplied-voltage characteristics are distinct boundaries	[32,51–54]
Reported renewable outcome	Hosting, curtailment, PV-origin delivery, losses, and battery throughput	An instantaneous voltage or capacity gain does not establish net delivered PV energy	[2,6,9,10,55]
Transferability boundary	Feeder impedance, climate, chemistry, charger, market, and connection code	Results remain conditional on their electrical, resource, and institutional setting	[50,56–58]

Table 4. Application of the analytical dimensions to ten illustrative sources.

Source	Binding Boundary	Battery or EV Duty	Validation Used	Renewable Outcome Used
[25]	LV feeder hosting	EV and BESS flexibility	Feeder simulation	Hosting change, not net annual PV energy
[26]	EV-integrated feeder	Placement and capacity	Optimization study	Siting effect, not a universal energy gain
[20]	Building and community BESS	SOC and degradation	Review	Battery operation, not feeder PQ
[21]	Grid-scale BESS	AI optimization	Systematic review	Techno-economic scope, not usable PV energy
[22]	Broad AI–BESS	Management and degradation	Comprehensive review	Method coverage, not PQ compliance
[27]	Distribution voltage	Safe reactive dispatch	Feeder simulation	Constraint satisfaction, not battery lifetime
[28]	Cell lifetime	V2G cycling	Cell experiment	Lifetime response, not feeder energy
[29]	Multi-battery allocation	Physics-informed control	Intelligent-control study	Constrained allocation, not feeder compliance
[30]	Laboratory microgrid	Hybrid storage buffering	Laboratory experiment	Transient behavior, not field hosting
[31]	MW flow-battery system	SOC and power allocation	Large-system model	Coordination result, not LV transfer

The evidence hierarchy is claim-dependent, not a universal score. Time-series studies can support annual energy and planning claims when feeder data and uncertainty are credible, while fast voltage, harmonic, resonance, protection, and converter claims may require electromagnetic-transient (EMT), controller-hardware-in-the-loop (HIL), power-hardware-in-the-loop, or prototype evidence. Pilot and field demonstrations add interoperability, operating-procedure, communication, customer, and institutional evidence that simulations cannot supply. This hierarchy is used to moderate the strength of conclusions rather than to rank technologies simply by the highest validation label reported in a paper.

3. System Boundary and Resource Roles in PV-Rich Networks

Figure 1 adopts a renewable-generation-centered boundary rather than treating PV, EVs, and BESS as parallel topics. PV is the generation resource whose usable output is to be maximized; EVs and BESS are time-varying electrical interfaces that can consume, shift, inject, or condition power; and the feeder/PCC imposes simultaneous compliance constraints. EV and storage technologies are included only to the extent that they change the amount, timing, and quality of PV electricity that can be accommodated by the distribution network.

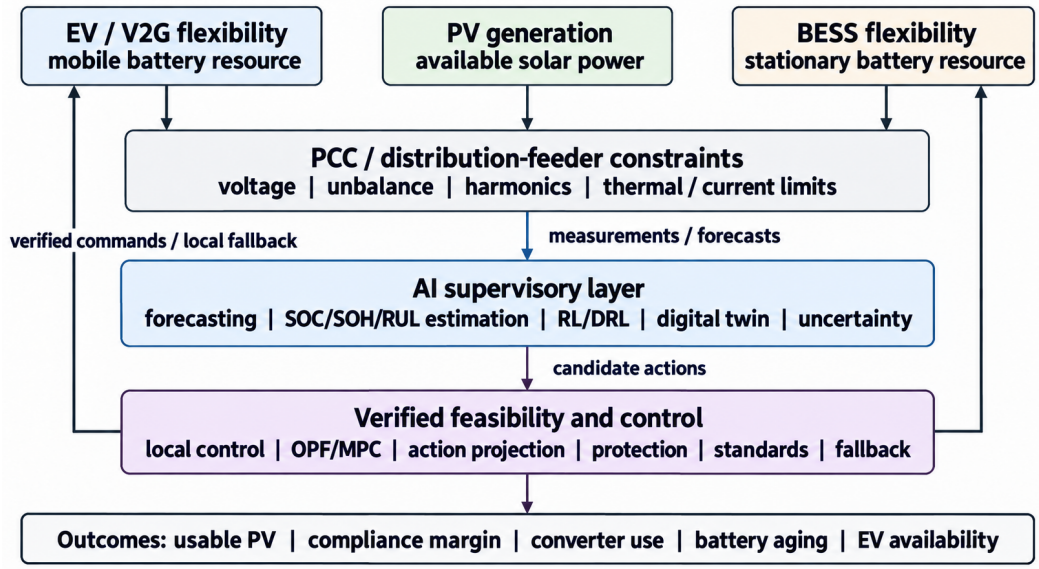


Figure 1. Renewable-generation-centered framework showing PV, BESS, and EV/V2G resource interactions, AI supervisory functions, and the binding electrical, battery, and mobility constraints. Abbreviations: AI, artificial intelligence; BESS, battery energy storage system; DRL, deep reinforcement learning; EV, electric vehicle; MPC, model predictive control; OPF, optimal power flow; PCC, point of common coupling; PV, photovoltaic; RL, reinforcement learning; RUL, remaining useful life; SOC, state of charge; SOH, state of health; V2G, vehicle-to-grid.

3.1. PV Generation and Feeder Hosting Constraints

Distribution-level PV is predominantly interfaced through power-electronic inverters, so the usable renewable-energy output depends on both the available irradiance and the admissible converter/network operating region. At low penetration, a grid-connected PV inverter is often represented as a controlled current source operating close to unity power factor. That simplification becomes inadequate when reverse power flow, voltage rise, weak-grid synchronization, converter-current saturation, or harmonic interaction becomes binding. Reported impacts also vary with phase connection and feeder topology, particularly where single-phase PV changes local voltage and phase balance [59,60]. Classical hosting-capacity studies already showed that feeder location and network voltage control can change the amount of generation that can be connected [1]; annual-duration approaches

further demonstrated that installed PV capacity and annual usable PV energy are not equivalent when curtailment is required to respect voltage limits [2]. For a renewable-energy assessment, the relevant quantity is the solar energy delivered within the feasible electrical envelope rather than nameplate penetration alone.

Most existing distribution PV operates in a grid-following mode. The inverter synchronizes to the PCC voltage, commonly through a phase-locked loop (PLL), while maximum-power-point tracking and DC-link control determine the available active-power command. In strong feeders this architecture is well established, but in weak feeders the interaction among synchronization dynamics, current limits, feeder impedance, and protection can become important. Grid-forming (GFM) control is consequently receiving attention because it can provide a voltage-source-like response and improve voltage/frequency support, yet weak-grid stability cannot be inferred from a single benchmark or from an unconstrained converter model [61]. A GFM inverter remains bounded by semiconductor current, DC-side energy, thermal limits, filter design, and ride-through/protection requirements. Virtual-synchronous-generator studies provide an additional converter-control baseline for damping and grid-support behavior [62], while PV converter research shows that DC-side power-decoupling design also shapes the realizable operating envelope [63]. These limits are central when the objective is to preserve PV generation during stressed operating conditions.

Voltage-management research has progressed from fixed power factor toward autonomous Volt–Var/Volt–Watt characteristics and coordinated active/reactive control. Local reactive-power control can reduce overvoltage without continuous communication, and feeder studies demonstrate the sensitivity of its benefit to network impedance and inverter capability [64,65]. Coordinated curtailment, PV–storage energy management, and high-penetration PV feeder models further show that the selected control boundary changes the apparent hosting benefit [66–70]. Hierarchical and coordinated schemes can allocate reactive power, curtailment, tap actions, and storage more selectively across a feeder [38,41]. Their principal advantage is system awareness; their principal weakness is dependence on network models, measurements, communications, and a defined fallback state. Reactive support is also not free. Near maximum PV output, converter apparent-power limits reduce the available Q headroom unless the inverter is oversized or active power is curtailed, and additional reactive current can increase feeder loss and converter temperature. These constraints explain why coordinated storage and inverter studies must be interpreted with their assumed tap control, feeder model, and device rating rather than through voltage deviation alone [6,9,10].

The PV hosting boundary is not purely a fundamental-frequency voltage problem. Experimentally validated work shows that pre-existing harmonic voltage distortion can reduce hosting capacity [3]; studies on high-PV urban and distorted distribution networks further show that harmonic propagation depends on phase allocation, background distortion, converter spectra, and frequency-dependent feeder impedance [4,5]. A PV installation can satisfy a local device test while the aggregated feeder still approaches a PCC distortion limit. Source-attribution methods become relevant when customer injections and upstream background distortion coexist [71]. These findings justify treating harmonic headroom, resonance, and measurement bandwidth as renewable-integration constraints rather than as post-design PQ checks.

Taken together, recent PV control developments reveal a recurring trade-off. Autonomous inverter functions are scalable and fast but have limited knowledge of system-wide constraints; coordinated controls can use network sensitivity more efficiently but introduce communication and model dependence; storage can recover curtailed energy but consumes finite SOC and lifetime; and active filtering can improve waveform quality while competing for converter current. Each method is evaluated by the additional

usable PV energy it can enable after these physical limits are represented, not by voltage improvement alone.

3.2. Electric-Vehicle Demand and Mobile Battery Flexibility

EV integration changes the PV operating envelope through demand timing, converter emissions, phase loading, and bidirectional flexibility. The first effect is temporal. Daytime workplace or destination charging can absorb local PV generation and reduce reverse power flow, whereas synchronized evening charging can increase feeder peak demand, voltage drop, transformer loading, and losses. Load models, smart-charging studies, and office-charging analyses show that charging coincidence, connection location, and user behavior must be represented explicitly when estimating these impacts [72–75]. Early PV–V2G studies showed that a parking facility with rooftop PV and bidirectional vehicles can enhance distribution capacity or reduce peak demand when the charging window overlaps the renewable-generation profile [7,36]. These benefits are conditional on vehicle presence, charger rating, driver energy requirements, and the location of the feeder constraint.

The second effect is converter-related. EV chargers are nonlinear power-electronic loads whose current spectrum is not fixed across all charger technologies or operating points. Modern active-front-end chargers can achieve substantially better power factor and lower low-order distortion than passive rectifier interfaces, but feeder-level PQ remains a function of aggregation, grid strength, background voltage distortion, and charging state [76,77]. Measurements demonstrate that harmonic current distortion can change with battery SOC during charging [46]; probabilistic feeder studies likewise show that EV and nonlinear-load uncertainty changes the distribution of PQ outcomes rather than producing one deterministic distortion value [33]. For residential networks, single-phase charger allocation also makes phase unbalance and neutral loading relevant even when three-phase aggregate power appears acceptable.

Smart charging uses this demand flexibility without requiring energy export from vehicle batteries. By shifting charging away from a constrained interval or toward local solar production, scheduling can reduce coincident demand and improve voltage conditions [73]. V2G extends the controllable range by permitting active-power export and, where the charger permits, reactive-power support. Aggregator formulations coordinate many vehicles to provide grid services while respecting charging-cost or availability objectives [8,78,79]. Real-time voltage-control studies use active and reactive EV flexibility to reduce voltage deviations [80–84], while distributed MPC exploits reactive V2G to coordinate multiple resources without relying on one central optimization step [39]. Disturbance-observer MPC and Volt/Var characteristic design continue this trend toward faster converter-aware support [42,85].

The electrical capability, however, is not equivalent to firm flexibility. A vehicle may be disconnected, the user-required departure SOC may be binding, a bidirectional charger may not be available, or additional battery throughput may be unacceptable without compensation. Distribution-system impact reviews and orderly-charging studies identify connection uncertainty, charging coordination, and network operating conditions as essential modeling inputs [86–90]. Planning and scheduling studies further show that network reconfiguration, stochastic demand, multiobjective dispatch, and coordinated charging/storage decisions alter the feasible service window [91–96]. Infrastructure-planning and solar-charging studies expose the conversion and siting trade-offs of mobile storage [97,98]. Lifecycle and second-life studies add chemistry, repurposing, and degradation constraints [99–102], while dispatch studies show how service schedules determine battery throughput and delivered grid value [103–105]. The renewable-energy measure is the additional PV energy absorbed or delivered, or curtailment avoided, after accounting for charging/discharging

loss, battery throughput, mobility constraints, and the timing of the network bottleneck. This distinction prevents V2G from being credited with renewable-hosting value when it only shifts energy at high lifecycle cost.

Experimental evidence supports the technical feasibility of converter-based EV support but also illustrates the validation gap. A three-phase off-board charger prototype has demonstrated practical grid-voltage regulation [48], and active harmonic-rejection control demonstrates that charger converters can participate in waveform support [40]. Field projects now extend the evidence beyond single-device laboratory work: the Australian Realising Electric Vehicle-to-Grid Services (REVS) trial involved 51 EVs connected through bidirectional chargers [50], and Project Sciurus deployed more than 300 domestic V2G units in the United Kingdom (UK) [106]. These demonstrations establish that aggregated V2G is no longer purely a simulation concept, while also exposing interoperability, customer participation, metering, communication, and jurisdiction-specific market constraints. For PV-rich feeders, EV flexibility is best represented as a bounded, probabilistic resource, not as guaranteed storage.

3.3. Stationary Battery Storage: Energy Shifting and Grid Support

BESS is the most direct bridge between renewable-energy time shifting and fast converter control. It can absorb PV energy during export-constrained periods, discharge later, provide reactive power, reduce voltage excursions, and coordinate with PV inverters and feeder regulators [6,9,10]. Storage technologies differ materially in response time, power density, usable energy, cycling behavior, and balance-of-plant requirements; these differences determine whether a resource is suited to fast PQ support, energy shifting, or neither [107–109]. Battery storage is the storage class emphasized because it is explicitly coupled to PV and EV operation in the target system.

At the feeder level, a BESS can support at least three different time scales. Fast converter control can provide reactive-power or waveform support without large energy exchange. Minute-scale active-power control can smooth ramps and relieve a temporary voltage or thermal constraint. Hour-scale scheduling can shift midday solar energy into later demand periods. These services compete for the same converter rating and, for active-power services, the same SOC window. Reserving apparent-power headroom for reactive or harmonic support can reduce simultaneous charging/discharging capability; reserving SOC for contingency support can reduce the amount of midday PV that can be stored; and aggressive active-power regulation can increase battery throughput and degradation.

This coupling is often hidden when studies report only an increase in hosting capacity. A storage controller may permit a larger installed PV nameplate but still curtail a substantial fraction of annual solar energy, or it may recover that energy at the cost of frequent cycling and conversion losses. A stronger evaluation reports the MW/MWh rating, SOC bounds, converter apparent-power limit, charging/discharging efficiency, degradation representation, priority among P/Q/PQ services, and the fraction of otherwise curtailed PV energy that is actually recovered. Sizing and dispatch studies often optimize losses, revenue, or a single service; their results cannot be treated as PQ-support evidence unless the converter and network constraints are also represented [110–112]. Distributed storage studies show that coordinated operation with transformer or feeder voltage control can mitigate PV-driven voltage rise [9,10], while coupled PV/BESS control can coordinate reactive support and energy storage [6]. Broader PQ-oriented storage control has also been used to address voltage, power-factor, and renewable/EV-related network issues [113].

The broader evidence separates three sources of storage value. EV and grid-integration reviews distinguish mobile and stationary storage by infrastructure, service, and interoperability requirements [114–118]. Renewable and hybrid-storage reviews instead emphasize

technology selection and the power/energy requirements of the target service [119–123]. Forecasting and renewable-smoothing studies show that dispatch value changes with forecast quality and hybrid-resource configuration [124–126]. Planning and optimization studies make the result conditional on the objective, uncertainty model, and network constraints [110–112]. Recent battery-system evidence further supports realistic SOC windows, cycling depth, C-rate, temperature, and aging instead of treating BESS power as a cost-free control input [47].

A useful renewable-energy indicator is incremental usable PV energy per unit of storage throughput together with the avoided network constraint. Active-power cycling changes stored energy and battery duty. Reactive or waveform support uses converter current and can also impose DC-side ripple, depending on phase configuration and power decoupling. Its battery impact therefore requires the interface model described in Section 3.4.

3.4. Battery Chemistry, Degradation, and Interface Architecture

Battery chemistry affects the sustainable power and energy envelope, but fast PQ response is delivered by the converter and its controller. Comparing chemistries by response time alone confounds electrochemical capability with inverter bandwidth. Table 5 therefore distinguishes repeated active-power duty from reactive or harmonic support, which can require substantial AC current with relatively little net battery-energy exchange. The comparisons are qualitative: cell design, temperature, SOC window, pack sizing, and manufacturer limits prevent a universal numerical ranking [24,34].

Table 5. Relative suitability of battery technologies for converter-mediated PQ support and energy shifting.

Technology	Fast PQ and Active-Power Duty	Energy Shifting	Principal Qualification
Lithium iron phosphate (LFP)	Suitable for repeated short active-power duties when current and thermal limits are respected; reactive/harmonic service remains inverter limited	Established stationary-storage option where cycling and thermal robustness are priorities	Lower energy density than nickel-rich cells can increase pack size; flat open-circuit voltage complicates SOC estimation; temperature and charging limits still apply [11,24]
Lithium nickel manganese cobalt oxide (NMC)	High energy density supports compact EV packs; sustained high-current duties require chemistry-specific thermal and aging assessment	Suitable for mobile storage and space-constrained installations	EV energy density does not establish economical stationary cycling; high SOC, temperature, and user reserve restrict V2G duty [24,28]
Lithium titanate (LTO)	Power-oriented cells can suit repeated active-power pulses and intensive cycling	Lower energy density can make bulk energy shifting less attractive where space and cost dominate	LTO denotes an anode material rather than a unique cathode chemistry; evaluate the complete cell, rated power, and pack cost [18,34]

Table 5. *Cont.*

Technology	Fast PQ and Active-Power Duty	Energy Shifting	Principal Qualification
Redox flow batteries	Fast electrical support requires an appropriately rated converter; repeated active support also depends on stack and electrolyte operating conditions	Independent stack-power and tank-energy sizing favors longer-duration stationary services	Pumps, auxiliary demand, electrolyte condition, and stack efficiency must enter net-energy accounting; not a mobile V2G resource [24,31]
Lead–acid	Short support is possible, but repeated deep cycling and high-rate duty require careful derating	Applicable where mature technology and initial cost outweigh weight and lifetime limitations	Depth of discharge, partial-SOC operation, temperature, and replacement frequency can dominate lifecycle cost [34]

Degradation models enter the comparison at three levels. Throughput or equivalent-cycle models assign a marginal wear cost to energy exchange and are convenient for dispatch but cannot distinguish two schedules with the same throughput and different SOC, temperature, or dwell time. Semi-empirical calendar-plus-cycle models capture these dependencies using fitted stress factors and, where appropriate, cycle-depth counting; their coefficients are cell- and duty-specific. Electrochemical or reduced-order physical models can represent internal limits and mechanisms more directly, at a greater identification and computation burden. Data-driven SOH models support online updating but inherit the coverage and uncertainty of their training data. A grid-service study should state its model, calibration domain, calendar-aging treatment, capacity-fade and resistance-growth measures, and how those measures change allowable current and usable energy [11,20,23].

The distinction has measurable consequences. Darikas et al. tested commercial 4.5 Ah lithium-ion cells using charger-derived V2G profiles at 5, 25, and 40 °C. Their comparison estimated approximately 0.62 full equivalent cycles per day for shallow 30–50% SOC cycling at a capacity-fade rate comparable to prolonged high-SOC storage. This is a cell-specific comparison with a high-SOC calendar-aging baseline, not a general wear-free V2G allowance [28]. In a separate simulation, Chen et al. reported up to 32% lower transient overshoot, 25–40% shorter settling time, and 12–23% lower peak battery-current stress at 60% SOH relative to non-SOH-aware control. These are modeled control-performance gains, not measured lifetime extensions [35]. Such results support including battery condition in control; they do not justify a universal degradation penalty or guaranteed service life.

Table 6 compares four experimental studies of battery aging under V2G or superimposed ripple duty; NCA denotes nickel cobalt aluminum oxide. The control simulation by Chen et al. is discussed above as a control-performance result and is excluded from this experimental table.

The battery management system (BMS) places an additional boundary on grid commands. Pack-level SOC and SOH estimates may conceal cell imbalance, local temperature, sensor bias, and unequal resistance. A dispatch optimizer must therefore receive the available charge/discharge limit, rather than assume the nameplate rating remains available. SOC-estimation uncertainty is particularly relevant for LFP voltage plateaus, while balancing, thermal derating, contactor protection, and charging restrictions can make an otherwise feasible feeder action unavailable. Learned state estimation complements these protections; it does not authorize overriding them [11].

Table 6. Experimental battery-aging evidence relevant to V2G and converter ripple.

Source	Reported Conditions	Reported Aging Observation	Limit of Use
Darikas et al. [28]	Commercial 4.5 Ah cells; charger-derived V2G profiles; 5, 25, and 40 °C; shallow 30–50% SOC cycling	About 0.62 full equivalent cycles per day, with a fade rate comparable to prolonged high-SOC storage	Cell-level comparison against a high-SOC calendar baseline; not a feeder lifetime guarantee
Dubarry et al. [127]	Commercial graphite/NCA cells; driving, charging, and additional grid-discharge schedules	Additional grid-discharge cycling accelerated degradation relative to the tested driving/charging schedules	Schedule- and chemistry-specific; neither a universal V2G penalty nor evidence about reactive-only service
Uddin et al. [128]	Fifteen cells; 1200 cycles; DC duty with superimposed AC at five frequencies	Frequency-dependent capacity/impedance degradation and greater cell-to-cell variation were reported	Ripple spectrum and test duty govern transfer; not a generic loss factor for every inverter
Bessman et al. [129]	28 Ah NMC/graphite cells; 21 A peak ripple at 1 Hz, 100 Hz, or 1 kHz; about 2000 cycles in one year	About 80% capacity remained; no additional capacity or power fade attributable to the tested ripple was detected	The measured capacity loss is total aging, not ripple-induced loss; results are confined to the tested cells and amplitudes

Temperature closes part of the same practical gap in low-voltage feeders. Ambient heat, enclosure design, and pack thermal resistance can force the BMS to reduce charge or discharge current before the electrical SOC window is exhausted. A controller that treats the nominal SOC limits as always available can therefore overstate both usable energy and fast PQ support during hot operating periods. The appropriate report is the thermally derated power together with the SOC window, not a single nameplate rating.

PV–BESS topology also changes the available actuator. In an AC-coupled installation, PV and storage typically have separate grid interfaces; their apparent-power limits and losses must be represented separately. In a DC-coupled installation, PV and storage exchange power through a common DC network, often with a shared grid inverter. This can permit DC-side PV charging without an intermediate AC conversion, but grid export, reactive support, and harmonic compensation compete within the shared inverter rating. DC–DC converter limits and DC-bus control remain relevant. Consequently, identical battery capacity does not imply identical curtailment recovery or PQ capability across AC- and DC-coupled systems [18,19]. Comparisons should identify the topology, conversion path, shared ratings, and auxiliaries before attributing a gain to chemistry or AI.

Phase configuration is material even when mean active power is zero. For sinusoidal single-phase voltage and current, with the voltage defining the cosine reference, instantaneous AC power is

$$p(t) = P + P\cos(2\omega t) + Q\sin(2\omega t), \quad (1)$$

where P and Q are average active and reactive power and ω is the fundamental angular frequency. The 2ω component must be buffered by the DC link, a decoupling circuit, or the battery interface; reactive-only operation can therefore impose battery ripple despite negligible mean energy transfer. Balanced sinusoidal three-phase power cancels this component across phases, although unbalance, distortion, and switching can reintroduce ripple. An LFP storage experiment examined twice-grid-frequency ripple through temperature, balancing, and round-trip efficiency [130]; power-decoupling designs change how much pulsating power reaches the DC source [63].

Battery ripple cannot be assigned a universal aging penalty. The contrasting experiments in Table 6 show that chemistry, ripple amplitude and frequency, DC bias, SOC, temperature, and interface filtering matter [128,129]. An additional heating estimate is $P_{\text{ripple,loss}} \approx \sum_f I_{b,f,\text{rms}}^2 \,\text{Re}\{Z_b(f)\}$, where $Z_b(f)$ is battery impedance at frequency f. This estimates electrical dissipation rather than capacity fade. PQ-support studies should report the battery-side spectrum and thermal response, and validate aging under representative duty instead of inferring it from AC-side reactive energy alone.

3.5. AI-Enabled Battery and EV Coordination

AI has a defensible role in this system boundary when it improves information, prediction, or sequential decision making that would otherwise be represented by fixed forecasts, static battery parameters, or inflexible scheduling rules. It does not enlarge converter current, feeder thermal capacity, or battery energy by itself. An AI-enabled architecture is technically meaningful only when the learned component operates inside explicit electrical and battery constraints and when a deterministic fallback remains available if data, communications, or the learned model become unreliable.

Recent reviews already cover AI-driven grid-scale BESS optimization and broad AI-enabled BESS functions across battery management, state estimation, fault diagnosis, predictive maintenance, thermal management, renewable integration, microgrids, and smart grids [21,22]. Replicating those broad taxonomies would not address the narrower grid-facing question considered here: AI is considered only when it changes the scheduling, observability, or robustness of stationary and mobile battery flexibility under an explicit PQ-constrained PV-integration objective. This distinction also separates the grid-facing synthesis from battery-management surveys centered on SOC/SOH/RUL prediction and cloud–edge digital twins [11].

Forecasting and battery-state learning can improve the information supplied to a constrained scheduler. Reinforcement learning instead selects sequential actions, as illustrated by mobile-storage routing [43]. Learning-assisted system scheduling and physics-informed battery allocation operate at different boundaries [12,29]; electrochemical charging models add battery-safety constraints [13].

For the present application, the distinction between *AI-enabled* and *AI-controlled* operation is material. AI can rank candidate actions, update forecasts, estimate hidden battery states, or adapt controller parameters while a projection, MPC/OPF, or rule-based layer enforces network voltage, converter current, SOC/SOH, mobility, protection, and interconnection limits. Comparative studies need to disclose the training and test domain, input observability, uncertainty treatment, inference or update time, hard action constraints, battery-aging model, communication assumptions, fallback action, and out-of-distribution tests. The relevant outcome is not prediction accuracy or cumulative reward in isolation, but the additional usable PV energy or compliance margin obtained after losses, battery throughput, degradation, and violation risk are accounted for.

In supervisory operation, learned forecasts or state estimates supply a constrained scheduler. In direct learned control, the policy proposes actions and a projection or safety layer corrects them before execution, as illustrated by distribution-voltage studies [27,131]. The comparison must identify which component enforces feasibility and how it responds when no admissible correction exists.

Method Taxonomy and Constraint Enforcement

AI functions differ in both their decision role and their safety burden. Supervised forecasting estimates PV, load, and vehicle availability for a separate scheduler. Battery-state learning updates SOC, SOH, or degradation parameters. Reinforcement learning (RL)

maps operating states to sequential decisions, while hybrid methods couple a learned policy or forecast to model predictive control (MPC) or optimal power flow (OPF). Physics-informed learning penalizes inconsistency with physical equations during training. These functions require different evidence: forecast accuracy must be connected to dispatch benefit, and dispatch benefit must be evaluated under the same battery, converter, and network limits as the baseline.

Constraint enforcement cannot be inferred from the word "safe" or from a reward penalty. An action projection solves for an admissible command closest to the proposed action. A safety layer corrects actions using a modeled or learned constraint response, whose validity depends on model error and update delay [27,132]. A constrained Markov decision process (CMDP) instead places limits on accumulated or expected costs during policy optimization [133]; satisfaction of those limits does not generally guarantee every instantaneous voltage, current, or temperature limit. A physics-informed loss likewise encourages consistency without necessarily enforcing all inequalities at execution. Table 7 separates these approaches and the evidence needed for PQ-sensitive operation; Table 8 compares representative applications and their validation limits.

Table 7. AI decision functions and approaches to constraint enforcement.

Approach	Role	Constraint Mechanism	Qualification for PQ Operation
Forecasting or state estimation	Inputs to MPC/OPF or rule-based dispatch	Feasibility resides in the downstream controller	Report forecast/state uncertainty and resulting compliance, energy, and battery-duty effects [11]
Action projection	Correct a learned command before execution	State-dependent feasible set; potentially coupled network and device inequalities	Validate the set against nonlinear/unbalanced operation, stale measurements, and infeasibility; simple power clipping is insufficient
Safety layer	Correct actions using estimated constraint response	Analytical or quadratic-programming correction	Safety is conditional on constraint-model accuracy and remaining feasible action; retain deterministic fallback [27,131,132]
CMDP/constrained policy optimization	Learn under explicit cost budgets	Expected or cumulative constraint costs	Report per-step violations separately; expected-cost satisfaction is not a conformance test [133]
Hybrid RL–MPC	Combine adaptive decisions and predictive feasibility	Explicit controller constraints plus learned objectives/actions	Disclose coupling, horizon, solve time, aging assumptions, and fallback; feasibility depends on the predictive model and constraint set
Physics-informed learning	Improve physical consistency	Conservation or state-equation residuals in training	Residual accuracy does not certify hard voltage/current or BMS limits at execution [29]

Table 8. Representative AI studies: reported function, validation, and limits of the claim.

Source	Method and Boundary	Reported Evidence	What Is Not Established
Kou et al. [131]	Deep deterministic policy gradient with safety layer; distribution voltage control	Numerical studies on modified IEEE systems; voltage constraints and power-loss reduction	Field operation, battery-aging benefit, and harmonic/PCC compliance
Gao and Yu [27]	Model-augmented RL with quadratic-programming safety layer; Volt–Var control	Simulated IEEE feeders; improved constraint satisfaction during training	Safety under arbitrary topology changes or complete PQ compliance
Ding et al. [43]	DRL route and charge/discharge decisions for mobile storage	Numerical network/transport optimization	Mobile storage routing is not equivalent to EV-user availability or measured feeder PQ
Tong et al. [12]	Learning-assisted multi-energy and battery–grid scheduling	Hourly system case study of energy balancing and switching activity	Hourly dispatch does not validate fast PQ response or electrochemical health
Al Qwaid et al. [13]	Attention-enhanced proximal policy optimization (PPO); battery charging	Single-particle electrochemical simulation; mean plating overpotential +0.023 V versus −0.015 V for baseline PPO	Modeled plating margin, not measured capacity retention or feeder compliance
Akinwola and Alkuhayli [29]	Physics-informed multi-battery PV charge allocation	MATLAB/Simulink R2023a comparison: final SOC variance 0.08% versus 0.65% for MPC; settling time 8.2 versus 14.3 s	SOC equalization and transient settling do not establish field/PCC harmonic compliance

The audited AI examples establish algorithmic and simulated control capability, with uneven treatment of battery duty and PQ metrics. No audited source demonstrates the complete combination of AI-controlled PV–BESS–EV operation in an actual distribution system, independently assessed PQ compliance, battery-health limits, and long-duration net-PV recovery. Field deployment of some grid-support functions is well established in Section 6.3, but those projects do not document that complete AI claim. This is an evidence gap within the audited set, not proof that no such deployment exists elsewhere.

3.6. Battery and EV Flexibility Across Operating Time Scales

Battery flexibility depends on service duration. Sub-cycle to second-scale PQ support is constrained by converter bandwidth, current, thermal margin, and DC-side ripple. Minute-to-hour dispatch additionally depends on usable energy, SOC, conversion efficiency, forecasts, and accumulated wear. V2G adds connection and departure-energy constraints. Table 9 relates each service to these resource limits.

Temperature, SOC, and cycle depth affect V2G aging [23,28]; compensation and participation affect its economics [37]; and parking duration and demand patterns affect PV–BESS sizing at charging facilities [55]. These dependencies should be modeled explicitly rather than absorbed into a generic flexibility factor.

Table 9. Battery and EV services for PQ-constrained PV integration: resource limits and representative evidence.

Service	Primary Electrical Action	Target Battery and Converter Duty	Primary Modeling Risk	Evidence
PV energy shifting	Charge during excess PV and discharge when the feeder can accept power	SOC window, usable energy, charge/discharge efficiency, throughput, temperature, and degradation	Hosting gain can be obtained at the cost of heavy cycling, losses, or insufficient energy capacity	[6,34,55]
Reactive voltage support	Inject or absorb reactive power to alter feeder voltage	Converter current and thermal headroom; battery energy exchange may be small but auxiliary losses remain	Apparent-power saturation can reduce simultaneous active-power charging or discharge capability	[6,9,10]
Ramp and active-power smoothing	Charge or discharge over seconds to minutes to moderate net power ramps	Power rating, SOC reserve, throughput, efficiency, control bandwidth, and repeated cycling duty	Fast smoothing may consume battery life without recovering substantial curtailed PV energy	[34,47,108]
V2G flexibility	Shift charging or export active/reactive power from connected EVs	Vehicle connection, bidirectional charger rating, departure energy, SOC/SOH, wear, and user participation	Treating an uncertain mobile resource as firm storage overstates available feeder support	[7,8,23,28]
Harmonic or multifunctional support	Allocate converter current to waveform compensation while maintaining the fundamental service	Harmonic-current share, fundamental current, thermal margin, filter design, and controller bandwidth	Independent attribution of full converter capacity to active, reactive, and harmonic services violates current sharing	[40,45,134]

For a time-series assessment, the renewable-energy consequence should be expressed as an integrated quantity rather than inferred from one favorable snapshot or an installed-capacity limit. Two quantities are distinguished. Gross accepted PV energy is

$$E_{\mathrm{PV,gross}} = \sum_{t} \left[P_{\mathrm{PV,avail}}(t) - P_{\mathrm{curt}}(t) \right] \Delta t, \tag{2}$$

where $P_{\mathrm{PV,avail}}(t)$ is available PV power and $P_{\mathrm{curt}}(t)$ is curtailed PV power. Gross acceptance is useful for identifying curtailed energy, but it should not be reported as delivered renewable energy when storage losses are material. A complementary boundary is therefore

$$E_{\mathrm{PV,net}} = \sum_{t} \left[P_{\mathrm{PV,direct}}(t) + P_{\mathrm{PV,dis}}(t) - P_{\mathrm{aux,PV}}(t) \right] \Delta t, \tag{3}$$

where $P_{\mathrm{PV,direct}}$ is PV power delivered directly to local load or the grid, $P_{\mathrm{PV,dis}}$ is PV-origin energy subsequently delivered from storage after discharge conversion losses, and $P_{\mathrm{aux,PV}}$ is auxiliary consumption assigned to that PV–storage service. PV energy remaining in storage at the end of the assessment horizon is reported separately unless the study adopts and states a terminal-energy accounting convention. Terminal SOC should not be given the same value as energy delivered to load or the grid. If a study values residual stored energy,

it should state the valuation convention, report the terminal SOC and residual energy explicitly, and must not also count that residual as delivered PV energy. This separation prevents a storage strategy from receiving credit for energy that entered the storage interface but was lost or remained unavailable for useful delivery.

The balance point for Equation (3) is the common AC bus at which local load receives energy and grid export is metered. Direct PV and battery discharge must be referred to that same bus, with applicable conversion and feeder losses included; gross PV capture uses its separately declared PV measurement plane. When the battery also charges from the grid, an explicit attribution convention is needed. Under proportional mixing, separate stored-energy inventories track PV-origin and grid-origin charging after charging losses. For positive stored energy $E_{b,t}$, the PV share $\alpha_t = E_{b,\mathrm{PV},t}/E_{b,t}$ gives $P_{\mathrm{PV,dis},t} = \alpha_t P_{d,t}$; discharge from an empty store is prohibited. Discharge and storage losses are allocated in the same proportion. Initial stored energy of unknown origin receives no PV credit, grid charging never becomes PV-origin energy, and auxiliary consumption is deducted only if it has not already been netted from the metered flows. This is a declared accounting convention, not physical identification of electrons.

For an accounting illustration, suppose 10 kWh of PV reaches that bus: 6 kWh serves load directly and 4 kWh charges an initially empty idealized store; another 2 kWh is charged from the grid. With 95% efficiency in each direction and no auxiliaries, the PV and grid inventories become 3.8 and 1.9 kWh. Full discharge delivers 3.61 kWh of PV-origin energy and 1.805 kWh of grid-origin energy, returning the store to its initial inventory. Delivered PV energy is $6 + 3.61 = 9.61$ kWh, rather than 11.415 kWh of mixed-source delivery or 10 kWh of gross capture. Empty initial/final inventory simplifies the arithmetic; it is not a recommended battery SOC range or a reported project result.

A consistent comparison reports the balance point, gross PV capture and curtailment, net PV-origin delivery, grid charging, conversion/auxiliary losses, initial/final SOC and provenance, battery throughput, and the limiting PQ metric with its assessment interval. Baseline and controlled cases should use the same horizon, weather/load data, and terminal-energy rule.

Battery state must be carried between time steps so that energy shifted in one interval cannot be reused without accounting for charging and discharging. An energy-state representation avoids changing the state variable merely because usable capacity changes with state of health or temperature [6,9,10,34]:

$$E_{b,t+1} = E_{b,t} + \eta_c P_{c,t} \Delta t - \frac{P_{d,t} \Delta t}{\eta_d}, \qquad \mathrm{SOC}_t = \frac{E_{b,t}}{E_{\mathrm{cap},t}}, \quad \mathrm{SOC}_{\min} \le \mathrm{SOC}_t \le \mathrm{SOC}_{\max}, \tag{4}$$

where $E_{b,t}$ is stored battery energy, $E_{\mathrm{cap},t}$ is the available capacity used for SOC normalization, $P_{c,t}$ and $P_{d,t}$ are charging and discharging power, and η_c and η_d are the corresponding efficiencies. A study that allows $E_{\mathrm{cap},t}$ to vary with SOH or temperature should state that model separately from the energy balance. When lifetime claims are made, throughput should also be defined explicitly, for example, as charge-plus-discharge energy or equivalent full cycles, and the degradation model should identify chemistry, temperature, C-rate, depth of discharge, and calendar-aging assumptions [23,28,47].

For a multifunctional converter, active-power transfer, reactive-power support, and harmonic compensation compete for finite semiconductor current and thermal capability. A simplified root-mean-square current-sharing envelope, consistent with converter-current allocation studies [40,45,134], is

$$I_1^2 + \sum_{h=2}^{h_{\max}} I_h^2 \le I_{\max}^2, \tag{5}$$

where I_1 is the fundamental current, I_h is harmonic current at order h, and I_{max} is the applicable current limit. This is a screening envelope, not a semiconductor thermal model. Experimental and control studies show that harmonic compensation and active grid support are constrained by converter design and available current headroom [40,45,134]; manufacturer thermal, modulation, filter, and protection limits can produce a smaller feasible region. Figure 2 places these electrical and battery limits in the energy-accounting path from available solar resource to usable PV energy.

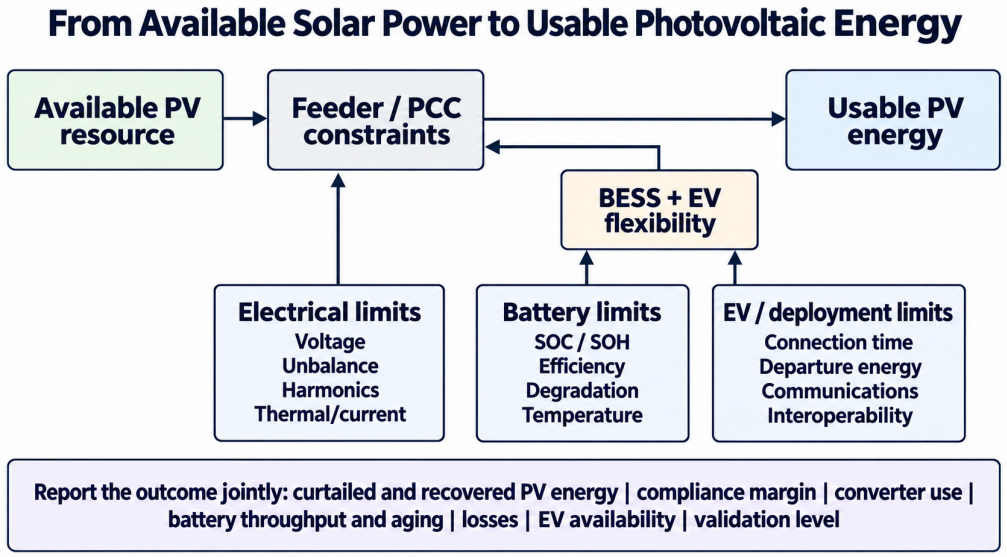


Figure 2. Constraint chain from available solar resource to usable PV energy. Electrical limits, battery limits, and EV/deployment conditions must be evaluated jointly so that recovered PV energy is not credited independently of battery throughput, losses, availability, or compliance margin. Abbreviations: BESS, battery energy storage system; EV, electric vehicle; PCC, point of common coupling; PV, photovoltaic; SOC, state of charge; SOH, state of health.

4. Power-Quality Mechanisms Limiting Usable PV Generation

Usable PV generation can be limited by several coupled electrical mechanisms, including voltage excursions, unbalance, waveform distortion, resonance, converter-current saturation, and thermal loading. The following subsections relate each mechanism to PV curtailment and to the specific BESS or EV flexibility that can relieve it.

4.1. Voltage Rise, Voltage Drop, Rapid Voltage Change, and Flicker

For a simple radial equivalent with resistance R, reactance X, net active-power injection P, reactive-power injection Q, and voltage magnitude V, a first-order steady-state voltage-change approximation is as follows [1,64]:

$$\Delta V \approx \frac{RP + XQ}{V}. \quad (6)$$

Here, positive P and Q denote net injection toward the feeder. Equation (6) explains why active-power export can create significant voltage rise in resistive low-voltage (LV) feeders and why the effectiveness of Q control changes with feeder resistance-to-reactance (R/X) ratio. Feeder studies identify phase shifting, reverse power flow, and location-dependent voltage sensitivity as distinct causes of the observed voltage rise [135–138]. Local and combined active/reactive inverter controls exploit that sensitivity with different information requirements [64,65,139]. Hierarchical and coordinated schemes extend the control boundary to storage and multiple feeder devices [6,38,140]. Forecast-aware curtailment and overvoltage-prevention methods address a different operating trade-off: they exchange

active energy for voltage margin [141–144]. The approximation should not be used as a substitute for an unbalanced nonlinear power flow when phase coupling, tap action, voltage-dependent load, or converter limits are material.

PV ramps, cloud transients, EV charging steps, and abrupt BESS dispatch can also create rapid voltage changes. Repeated voltage fluctuations may be evaluated through flicker indices when the disturbance falls within the applicable measurement framework. IEC 61000-4-15 specifies flickermeter behavior, whereas IEC 61000-4-30 defines measurement methods for PQ parameters including flicker and rapid voltage changes [52,145]. Studies of PV and charging networks also show that the outcome depends on feeder strength, charging events, generation variability, and the temporal aggregation used for assessment [56,57,146,147]. For twelve consecutive short-term severity values, the conventional long-term flicker index is

$$P_{\mathrm{lt}} = \left(\frac{1}{12} \sum_{i=1}^{12} P_{\mathrm{st},i}^{3} \right)^{1/3}. \tag{7}$$

Here, $P_{\mathrm{st},i}$ is the ith short-term flicker severity and P_{lt} is the long-term flicker severity. Equation (7) follows the standardized aggregation framework in IEC 61000-4-15 [145]. It is a measurement aggregation rule rather than a universal PV ramp limit. A renewable-integration study should not infer compliance from an arbitrary voltage-change threshold when the applicable requirement is based on a standardized statistic and assessment interval. Conversely, not every PV ramp should be described as perceptible flicker; the terminology and metric should follow the relevant measurement definition.

EV charging changes the sign and timing of net P. Daytime charging can reduce PV export and overvoltage, whereas uncontrolled evening charging can deepen voltage drop and transformer stress. Coordinated charging and V2G can reshape this envelope [7,39,73]. The control objective is bidirectional: release PV export capacity during high generation without creating undervoltage or charging-service failures during periods of high demand.

4.2. Voltage Unbalance, Phase Allocation, and Neutral Current

Residential PV and EV chargers are frequently single-phase, so a balanced three-phase model can conceal the actual hosting constraint. Phase allocation, grounding, and the local mix of PV and charging loads determine whether the negative- and zero-sequence components become material [60,148–150]. A standard sequence-component indicator is the voltage-unbalance factor (VUF) [52]:

$$\mathrm{VUF} = \frac{|V_2|}{|V_1|} \times 100\%, \tag{8}$$

where V_1 and V_2 are the positive- and negative-sequence voltage magnitudes. Equation (8) follows the sequence-component definition used for standardized PQ assessment [52]. Unbalance influences customer voltage, rotating equipment, converter control, and harmonic propagation because sequence impedances are different. Phase-aware connection planning, phase-aware smart charging, and coordinated reactive support can create hosting value that does not appear in a balanced feeder study.

Nonlinear single-phase converters also inject triplen harmonic components that can add in the neutral conductor instead of canceling. The resulting neutral current depends on the charger/inverter spectrum, diversity, conductor configuration, and phase allocation; it should not be generalized from one device measurement. Stochastic and probabilistic feeder studies are useful because charging coincidence and connection location determine the aggregate result [33,72,77]. For PV/EV-rich residential feeders, phase allocation and neutral loading should be included whenever conclusions are made about thermal headroom or PQ compliance [59,60,148,149].

4.3. Harmonics, Interharmonics, Supraharmonics, Resonance, and Source Attribution

Harmonic compliance is a network interaction problem. IEEE 519 frames harmonic control at the PCC [32], while IEC 61000-4-7 defines instrumentation and grouping for harmonics/interharmonics and IEC 61000-4-30 defines broader PQ measurement methods [52,53]. A device that satisfies an equipment-level emission test does not guarantee feeder-level compliance because the resulting waveform depends on aggregate converter spectra, background voltage distortion, frequency-dependent network impedance, resonance, and operating state [151–156].

Voltage and current total harmonic distortion (THD) are defined over the stated assessment bandwidth as follows [52,53]:

$$\mathrm{THD}_V = \frac{\sqrt{\sum_{h=2}^{h_{\max}} U_h^2}}{U_1} \times 100\%, \tag{9}$$

$$\mathrm{THD}_I = \frac{\sqrt{\sum_{h=2}^{h_{\max}} I_h^2}}{I_1} \times 100\%, \tag{10}$$

where U_h and I_h are the rms voltage and current components at harmonic order h, U_1 and I_1 are the fundamental rms voltage and current, and $h_{\max}$ is the highest harmonic order included in the assessment. For network-current assessment, IEEE 519 uses total demand distortion (TDD), which can be expressed as follows [32]:

$$\mathrm{TDD} = \frac{\sqrt{\sum_{h=2}^{h_{\max}} I_h^2}}{I_L} \times 100\%, \tag{11}$$

where I_L is the maximum demand load current at the PCC under the applicable assessment convention. Unlike instantaneous current THD, TDD uses a demand-current basis and therefore avoids inflating the ratio solely because the fundamental current is small.

IEEE 1547-2018 instead specifies total rated-current distortion (TRD) at the reference point of applicability (RPA) for DER current-distortion assessment [51]. Using the prescribed measurement bandwidth,

$$\mathrm{TRD} = \frac{\sqrt{I_{\mathrm{rms}}^2 - I_1^2}}{I_{\mathrm{rated}}} \times 100\%, \tag{12}$$

where I_{rated} is DER rated current referred to the RPA and I_{rms} includes harmonic and interharmonic components. TRD differs from both current THD and Equation (11) in normalization and, for the integer-harmonic sum shown there, spectral content. IEEE 1547 excludes distortion attributable to pre-existing area-system voltage distortion under its assessment rules. Its TRD limit is 5%, subject to the standard's provisions, including agreed active-filtering operation. A TDD value at a customer PCC cannot simply be relabeled as DER TRD.

A compact Thevenin-type harmonic-network representation used in impedance-aware assessment [3,4,157,158] is

$$V_h = Z_h I_h + V_{h,\mathrm{bg}}, \tag{13}$$

where V_h is the harmonic voltage, I_h is the injected harmonic current, Z_h is the feeder harmonic impedance, and $V_{h,\mathrm{bg}}$ is the background harmonic voltage. This simplified relation makes the location and operating-state dependence explicit: identical current injection can produce different harmonic voltages. Experimentally validated PV work confirms that background harmonic voltage can reduce hosting capacity [3], and feeder studies show that high PV penetration and passive-filter tuning can alter harmonic hosting and resonance behavior [4,5]. Related work on measured distortion, PV harmonic propagation,

and nonlinear-load interactions likewise supports an impedance- and boundary-aware interpretation [157–161]. Source-attribution methods are needed when utility background distortion and customer converter emissions coexist [71].

Resonance is especially important when shunt capacitance, filters, cables, and grid inductance create a high-impedance region near a converter emission. A simplified parallel-resonance estimate used for initial impedance screening [5,158] is

$$\omega_{\text{res}} \approx \frac{1}{\sqrt{L_{\text{grid}} C_{\text{shunt}}}}, \tag{14}$$

where ω_{res} is the estimated resonant angular frequency, L_{grid} is the equivalent grid inductance, and C_{shunt} is the shunt capacitance. The actual resonance requires the complete frequency-dependent network and converter model. The practical implication is that passive filtering can increase harmonic-constrained PV hosting in one feeder [5] but can be ineffective or adverse after the network impedance changes.

The THD expressions above apply to integer harmonics and do not aggregate interharmonics. The reviewed spectrum also extends beyond conventional low-order harmonics. Interharmonics occur at noninteger multiples of the fundamental, and conducted emissions in the 2–150 kHz range are commonly discussed as supraharmonics. IEC 61000-4-30:2025 includes measurement treatment for emissions across the 2–150 kHz range, while IEC 61000-4-7 remains central to harmonic/interharmonic grouping at lower frequencies [52,53]. Charger measurements show that the spectrum changes with topology, charging power, state of charge, and the local voltage waveform [46,162,163]. Harmonic-control studies add the effects of filtering, compensation bandwidth, and charger operating state [134,164–166]. The assessment must state its bandwidth; low-order THD cannot summarize the full converter spectrum.

4.4. DC Injection, Protection Interaction, and Converter-Current/Thermal Coupling

Transformerless converters can produce a small DC component because of sensor offset, modulation asymmetry, or control bias. Persistent DC injection can bias magnetic components and increase thermal stress. The admissible level and test method must be taken from the applicable interconnection/product requirement; no universal percentage is assigned across standards or jurisdictions. IEEE 1547 and its 2020 amendment are used here for distributed energy resource (DER) interconnection behavior, not as a universal rule for EV chargers or all customer equipment [51,167]. Protection and ride-through evidence must be interpreted with feeder fault level, protection settings, inverter current limiting, and the active-power reduction strategy applied during voltage sags [168–173]. Distribution-network studies quantify how PV and EV integration changes line loss, voltage drift, and feeder loading [174–177]. Peak-demand and integrated PV/EV studies add the dependence on charging demand, storage, and demand response [178,179], while PQ indices and distorted-network assessments address waveform-related loading [180,181]. Thermal headroom therefore requires direct assessment of conductor and transformer ampacity, neutral loading, harmonic losses, and converter derating.

PQ support can also shift the binding constraint from voltage to converter current. With an apparent-power rating S_{max}, a standard fundamental-frequency converter-capability boundary [6,45] is

$$P^2 + Q^2 \leq S_{\text{max}}^2. \tag{15}$$

Equation (15) is a simplified fundamental-frequency converter-capability boundary. It shows that operation near maximum PV active power leaves less reactive-power headroom unless the inverter is oversized or active power is curtailed. Harmonic compensation also consumes current capability and can increase switching and thermal stress [40,45,134].

For BESS and V2G, the feasible region is further reduced by SOC, energy reserve, mobility, and charging constraints. A controller should report its feasible P/Q/harmonic-current region under saturation rather than an unconstrained ancillary-service capability.

Table 10 summarizes how these mechanisms translate into renewable-generation consequences and identifies the associated battery or converter burden. The organization is intentionally mechanism-based because the same mitigation can release one constraint while tightening another through current saturation, additional cycling, altered harmonic impedance, or reduced energy reserve.

Table 10. Coupled PQ mechanisms limiting usable PV generation and associated evidence.

PQ Mechanism	Impact on Renewable Generation	EV and BESS Coupling	Core Mitigation Strategy	Standards and Evidence Basis
Steady-state voltage rise/drop	PV curtailment or reduced hosting when voltage limits bind	charging may absorb export; BESS/V2G can shift or inject P/Q	local or coordinated P/Q control, scheduling, storage	[1,2,39,64]
Rapid voltage change/flicker	limits acceptable ramping or switching behavior	charger/BESS steps can add or counter voltage changes	ramp-rate control, scheduling, fast inverter support	[52,145]
Unbalance/neutral loading	phase-specific voltage or thermal limit can bind before three-phase capacity	single-phase charging and V2G alter phase loading	phase allocation, phase-aware scheduling and control	[16,33]
Harmonic distortion/ resonance	harmonic headroom can reduce PV hosting despite acceptable fundamental voltage	charger/BESS spectra add to or compensate distortion	impedance-aware assessment, active/passive filtering, source attribution	[3–5,71]
Converter-current/ thermal limit	Q or harmonic support can force active-power curtailment	BESS/V2G services compete for the same converter rating	explicit current, thermal, SOC and service-priority constraints	[6,34,40]

5. Control Under Coupled Network and Battery Constraints

Table 11 provides a source-referenced comparison without treating heterogeneous case-study results as a universal performance ranking. The comparison focuses on the renewable/PQ benefit, binding implementation constraints, and failure modes that can invalidate an otherwise favorable result. More fundamentally, a controller should be judged by the constraint it releases and the cost of maintaining that release: a voltage reduction that increases feeder current, a harmonic intervention that exhausts converter headroom, or a BESS schedule that recovers curtailed PV only through excessive cycling is not a complete renewable-integration benefit. Comparisons require an explicit baseline, time horizon, feeder and PCC boundary, device saturation model, fallback behavior, and accounting of curtailed/recovered PV energy, losses, and battery throughput. This criterion prevents nominal control performance from being mistaken for transferable operating value.

Table 11. Control strategies for expanding the feasible PV operating region.

Control Strategy	Renewable and PQ Benefits	Binding Implementation Constraints	Potential Operational Failure Modes	Evidence
Local Volt–Var/droop	Fast autonomous voltage support with low communication burden	Inverter current and reactive-power headroom; local sensing; interaction among many devices	Local actions can increase losses or move voltage problems elsewhere in the feeder	[1,49,64]
Coordinated Volt–Var/Volt–Watt	Allocates reactive power and curtailment system-wide and can increase PV hosting	Telemetry, model or sensitivity accuracy, communication delay, and curtailment allocation	An optimizer solution may become infeasible or ineffective when telemetry is delayed or the network model is inaccurate	[6,38,41,142]
Centralized OPF/MPC	Explicitly coordinates multiple network, converter, and battery constraints over an operating horizon	State estimation, communications, computation time, forecast quality, and credible device models	A nominal optimum can fail when mobility, SOC, converter headroom, or feeder conditions differ from the assumed state	[41,81,112,182]
Distributed MPC	Reduces dependence on one central optimizer and can coordinate geographically dispersed EV flexibility	Neighbor or agent communications, convergence tolerances, asynchronous updates, and data availability	Communication degradation or poor convergence can fragment the feasible region and invalidate the coordinated service	[7,39,42,183]
BESS dispatch	Absorbs solar export and provides active or reactive support across different operating time scales	SOC, SOH, degradation, converter rating, losses, thermal limits, reserve requirements, and efficiency	A reported hosting gain may be purchased through excessive cycling, battery-health loss, or low net renewable-energy recovery	[6,9,35,47,55]
AI-enabled supervisory coordination	Forecasts, state estimates, and adaptive BESS/EV scheduling	Training domain, uncertainty, telemetry, inference time, hard constraints, and fallback	Apparent gains can depend on unseen violations, weak baselines, or omitted degradation	[11–13,43]
V2G aggregation	Adds mobile active and reactive power flexibility and can align charging demand with PV generation	Vehicle availability, user SOC/SOH, battery wear, charger interoperability, compensation, mobility reserve, and market access	Scheduled service becomes unavailable when vehicles disconnect, user energy requirements bind, or lifetime and compensation constraints are ignored	system/control: [7,8,36]; deployment: [50,106]; availability and lifetime: [23,28,37]

Table 11. *Cont.*

Control Strategy	Renewable and PQ Benefits	Binding Implementation Constraints	Potential Operational Failure Modes	Evidence
Active filtering/converter PQ support	Provides fast harmonic compensation and can improve waveform quality at the PCC	Converter current margin, switching and thermal stress, sensing bandwidth, filter design, and simultaneous fundamental-frequency services	Fundamental active/reactive service and harmonic compensation compete for finite semiconductor current and thermal capability	[40,134,164,184]

5.1. Autonomous Local Control

Local Volt–Var and Volt–Watt functions retain operation during loss of upstream communication. However, correcting local voltage can increase current and losses elsewhere, and the first site to reach a curtailment threshold need not have the greatest sensitivity to the feeder constraint. Settings therefore require feeder-aware operating envelopes [1,64].

5.2. Coordinated and Optimization-Based Control

Hierarchical control, OPF, and MPC can coordinate voltage, thermal loading, curtailment, SOC, and EV availability [38,41,81]. Evaluation should disclose model and forecast errors, update interval, solve time, infeasibility handling, and fallback when telemetry is stale. Benchmark optimization alone does not validate the information and communication chain [185–187].

5.3. AI-Enabled Supervisory Control

The AI functions and safety mechanisms in Section 3.5 must be evaluated against a conventional controller with matching physical constraints. Mobile-storage routing and physically informed battery allocation demonstrate useful decision roles [29,43]; battery-state surveys identify uncertainty and transferability limits [11]. A convincing system comparison reports usable PV delivery and violations under forecast error, communication loss, and states outside the training domain.

Distributed coordination can reduce dependence on a single optimizer and exploit geographically dispersed EV reactive-power capability through distributed MPC [39,42]. It does not, however, eliminate communication requirements. Neighbor-to-neighbor exchange, convergence tolerances, asynchronous updates, and packet loss can determine whether the resulting solution remains feasible. Its value therefore lies in resilience and scalability under a specified communication model, not in an assumed reduction in data exchange.

Storage and V2G availability require power/energy ratings, efficiency, and cycling duty to be specified [34,108,109,188,189]. Active support uses stored energy; reactive support can also impose battery ripple unless the interface buffers the pulsating power. EV availability, user requirements, and charging coordination further restrict the service [8,39,75,190–192]. The energy-attribution convention in Section 3.6 applies when grid and PV charging coexist.

5.4. Harmonic Compensation and Hardware Support

Active filtering and multifunctional chargers can recover harmonic headroom within the shared current envelope of Equation (5). Studies address charger models, rectifier suppression, combined storage/filtering, and bidirectional architectures [193–198]; static synchronous compensator (STATCOM), distribution STATCOM (D-STATCOM), and adaptive

control studies supply related voltage/waveform evidence [199–202]. Passive filters require impedance checks because a network change can create a new resonance [5,40]. Selection should follow the binding disturbance, available hardware, and validated operating range.

6. Compliance, Validation, and Deployment

6.1. Compliance Boundary and Jurisdictional Scope

Table 12 distinguishes interconnection requirements, installation-level disturbance allocation, equipment emission limits, and measurement methods. IEEE 1547.9 applies IEEE 1547 to storage DER, including relevant bidirectional interfaces [203]. EN 50549-1 and -2 address generating-plant connection to low- and medium-voltage (LV/MV) networks, subject to national implementation [204,205]. IEC TR 61000-3-6 covers MV, high-voltage (HV), and extra-high-voltage (EHV) installation emission allocation; IEC TR 61000-3-14 addresses LV installations. IEC TR 61000-3-15 assesses LV dispersed-generation electromagnetic compatibility (EMC) requirements [206–208]. The latter is cataloged by IEC as a Technical Report (TR). These installation documents complement equipment limits and do not replace them. Battery safety and EV communication are separate boundaries under IEC 62619 and ISO 15118-20 [209–211]. Applicability requires the local connection code, adopted edition, operating mode, and measurement point to be stated.

Table 12. Principal standards referenced in the review and their assessment boundaries.

Standard/Code	Assessment Boundary	Required Conformance Evidence	Implications for Grid Integration
IEEE Std 519-2022 [32]	PCC harmonic environment	voltage/current spectra, demand-current basis, aggregation/operating condition	equipment compliance alone does not establish feeder/PCC compliance
IEEE Std 1547-2018 [51]	DER–area electric power system (EPS) interface at the RPA	performance category, settings, ride-through, and current distortion including TRD	rated-current normalization differs from PCC TDD; converter limits still apply
IEEE Std 1547.9-2022 [203]	Storage DER interconnection; applicable bidirectional modes	application of IEEE 1547 to storage operating modes, export capability, and connection arrangements	a storage application guide, not a substitute for equipment testing
EN 50549-1/-2:2019 + A1:2023 [204,205]	Generating plants on LV/MV networks, respectively	applicable plant category, protection and operational capabilities, and national implementation	European connection requirements must be mapped to the local network code
IEC TR 61000-3-6:2008 [206]	Distorting installations on MV/HV/EHV systems	planning levels, background distortion, and allocated emission contribution	installation allocation differs from an individual converter emission test

Table 12. *Cont.*

Standard/Code	Assessment Boundary	Required Conformance Evidence	Implications for Grid Integration
IEC TR 61000-3-14:2011 [207]	Disturbing installations on LV systems	harmonics/interharmonics, voltage fluctuations and unbalance, with system absorption capacity	supports site-specific allocation; does not prescribe a mitigation device
IEC TR 61000-3-15:2011 [208]	Low-frequency EMC of dispersed generation on LV networks	emission/immunity assessment and test context for single- and multi-phase converters	technical guidance rather than a universal interconnection limit table
IEEE Std 1547.1-2020 [212]	DER interconnection conformance testing	prescribed test configuration, procedures, and measured response for claimed IEEE 1547 functions	controller simulation does not replace equipment-level conformance evidence
IEC 61000-4-7 [53]	harmonic and interharmonic measurement	stated bandwidth, grouping and instrument method	comparisons require consistent spectral measurement definitions
IEC 61000-4-15/IEC 61000-4-30 [52,145]	flicker and broader PQ measurement	instrument class/method, aggregation interval, rapid-voltage-change (RVC) and flicker definitions	PV ramps or charger steps should be evaluated using the applicable standardized metric
IEC 61000-3-2/IEC 61000-3-12 [213,214]	equipment harmonic-current emission limits	rated input current, equipment category, test conditions, and applicable connection boundary	equipment-level emission compliance does not by itself establish feeder/PCC harmonic compliance
IEC 61000-2-2/IEC 61000-2-12 [215,216]	Compatibility levels on LV/MV public systems	network environment, disturbance quantities, and applicable compatibility levels	compatibility levels are distinct from equipment limits and allocated site emissions
IEC 62619:2022 [209]	safety of industrial secondary lithium cells and batteries, including stationary applications	applicable safety tests, battery design, and declared operating conditions	grid-service claims remain bounded by battery safety and operating limits
D ISO 15118-20:2022 + Amd 1:2026 [210,211]	EV–charging-station communication for bidirectional power transfer and DER services	interoperable communication functions, supported services, and security provisions	electrical V2G capability is not deployable without a compatible communication and service interface

Table 12. *Cont.*

Standard/Code	Assessment Boundary	Required Conformance Evidence	Implications for Grid Integration
EN 50160 [54]	characteristics of supplied voltage	applicable national adoption and monitoring interval	supply-voltage characteristics are not a substitute for DER equipment requirements

Market remuneration, flexibility procurement, stakeholder liability, tariff design, export rights, and cost allocation are more jurisdiction-specific than the underlying electrical equations. The Australian and UK projects discussed below show that dynamic export and V2G services can be implemented, but they do not establish universal payment rules or a globally harmonized grid-forming requirement. Any deployment must map the engineering control to the local interconnection code, metering and settlement arrangement, consumer agreement, responsible network actor, and allocation of curtailed-energy, degradation, and communication costs. A technically effective controller can still be unattractive when it secures voltage compliance through excessive PV curtailment, costly communication infrastructure, or uncompensated battery wear; conversely, a BESS or V2G action with a high direct cost can be justified when it recovers renewable energy, defers reinforcement, and delivers multiple verifiable services over its lifecycle. The electrical feasibility region must consequently be evaluated together with the commercial mechanism that makes the assumed flexibility available, while avoiding unsupported extension of IEEE/IEC/EN technical evidence into global policy claims.

6.2. Validation Evidence and Transferability

To avoid equating the volume of simulation literature with deployment maturity, the review attaches validation level to the claim being made rather than converting evidence into an unsupported numerical score. Figure 3 summarizes the claim-specific progression from planning studies to field deployment while preserving the distinction between feasibility, real-time implementation, interoperability, and operational transferability.

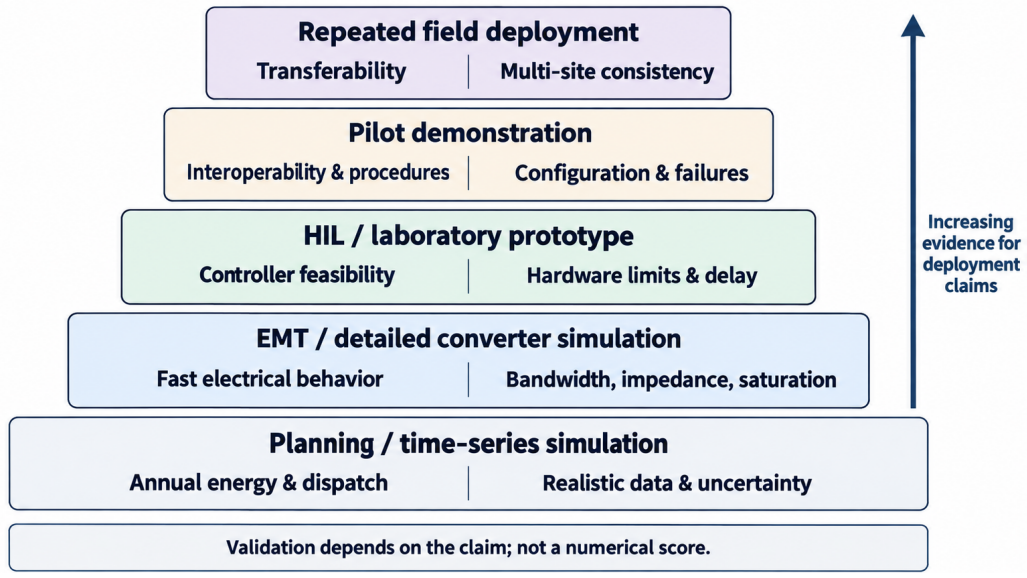


Figure 3. Claim-specific evidence maturity ladder used in the review. Higher levels add implementation and deployment evidence, but the appropriate endpoint depends on the claim and the ladder is not a numerical ranking of controller families. Abbreviations: EMT, electromagnetic transient; HIL, hardware-in-the-loop.

Validation evidence is discussed explicitly but is not converted into a numerical distribution unless every counted record and classification is supplied in a traceable audit trail. A validation label is used only when the study boundary and platform are explicit; title metadata alone are not used to infer maturity. Recent laboratory work provides a useful example: a PV–wind microgrid with battery–supercapacitor storage was evaluated experimentally against a battery-only baseline, linking transient DC-bus buffering to AC-side voltage behavior [30]. This distinction separates evidence for engineering feasibility from evidence for operational readiness. Benchmark and real-feeder simulation remain useful for planning claims, whereas fast converter, harmonic, protection, and communication claims may require electromagnetic-transient (EMT), controller- or power-hardware-in-the-loop (HIL), laboratory, pilot, or repeated field evidence. The appropriate endpoint depends on the claim: a planning-screening method does not require the same evidence as a sub-second closed-loop PQ controller. This conservative treatment deliberately avoids presenting an untraceable small-sample bar chart as if it were a census of the literature.

6.3. Field, Pilot, and Experimental Evidence

Table 13 separates field and pilot demonstrations from laboratory, prototype, and system-model evidence that is sufficiently specific to test the transferability logic developed in the preceding sections. The evidence level is therefore part of each entry and is not treated as interchangeable across rows. The entries are used to establish what has actually been demonstrated under stated technical and institutional conditions, not to imply universal transferability across feeders, jurisdictions, battery chemistries, charger populations, communication architectures, or market arrangements. In the project labels, NREL denotes the National Renewable Energy Laboratory, SCE denotes Southern California Edison, REVS denotes Realising Electric Vehicle-to-Grid Services, and VPP denotes virtual power plant; these abbreviations are retained only where they are the established project or industry names.

Table 13. Field, pilot, laboratory, and system-model evidence for PV hosting and battery–grid integration.

Project/Deployment	Technology and Validation Level	Reported or Supported Grid Capability	Transferability and Deployment Limits	Reference
NREL–SCE Fontana field demonstration	High-penetration PV with advanced inverter functions; utility field demonstration	Tested inverter functions on an operating distribution circuit with high PV penetration and connected local control behavior to feeder-level voltage and PV integration.	One utility circuit with project-specific feeder impedance, inverter population, monitoring, and operating procedures; the result is evidence of feasibility rather than a universal setting.	[49]
UK low-voltage PV–storage field trial	Customer-owned rooftop PV and small-scale storage; field PQ measurements combined with desktop network studies	Field measurements assessed coordinated storage operation and power quality. A separate modeled 100% storage-uptake case produced 4.1094% third-harmonic voltage against a 4.0% study limit when other nonlinear loads were included.	The 100% uptake and harmonic result are modeled extrapolations, not observations from full-penetration field deployment; the controller was not established as AI.	[217]

Table 13. *Cont.*

Project/Deployment	Technology and Validation Level	Reported or Supported Grid Capability	Transferability and Deployment Limits	Reference
REVS, Australia	51 EVs using bidirectional charging; fleet-scale pilot	Field availability evidence: 38 of 51 chargers had usable data and 29 had discharge data. In 2022, recorded discharge was 0.146 MWh versus 18.4 MWh imported; this is sparse contingency-service duty, not continuous regulation.	The trial comprised 51 bidirectional chargers; the final analytical dataset included 38 chargers, with discharge data available for 29. Australian regulatory conditions, market arrangements, charger technology, and customer participation limit direct transfer.	[50]
Project Sciurus, United Kingdom	More than 300 domestic V2G units; large residential pilot	Demonstrated household-scale bidirectional charging, customer behavior, data collection, aggregation, and portfolio operation at a scale beyond laboratory prototypes.	UK distribution-network connection rules, tariffs, domestic load patterns, and trial hardware are jurisdiction and technology specific.	[106]
Advanced VPP Grid Integration, South Australia	Distributed PV, batteries, and dynamic export limits; utility–aggregator demonstration	An 18-month field trial at 1000 sites increased available VPP export capacity from 5 MW to 6–8 MW during solar hours, with dynamic limits and communication-loss fallback. This is export capacity, not measured annual net PV-energy recovery.	Implementation depends on the utility/VPP interface, network models, communication availability, and Australian governance arrangements.	[58]
PV-coupled EV charging in low-voltage feeders	EV charging facilities coordinated with local PV; application study on LV feeders	Modeled how charging timing and location alter feeder loading and can improve local PV utilization when charging is coordinated with network conditions.	Results depend on feeder topology, charger penetration, driving/charging patterns, and assumptions regarding controllability and customer behavior.	[56]
Three-phase off-board EV charger voltage support	Bidirectional charger prototype; laboratory implementation	Demonstrated practical converter-based voltage regulation and showed that an EV interface can provide grid-support functionality beyond uncontrolled charging.	Prototype ratings, controller bandwidth, measurement filters, and laboratory network conditions do not establish fleet-scale availability or field interoperability.	[48]

Table 13. *Cont.*

Project/Deployment	Technology and Validation Level	Reported or Supported Grid Capability	Transferability and Deployment Limits	Reference
Active harmonic rejection in EV charging	Converter control with experimental waveform support	Demonstrated that charger power electronics can participate in harmonic mitigation, supporting the multifunctional-converter interpretation adopted in the synthesis.	Harmonic performance depends on grid impedance, background distortion, filter design, current headroom, switching frequency, and the measurement boundary.	[40]
Lab-scale renewable microgrid with hybrid storage	PV–wind generation with battery–supercapacitor storage; analytical and laboratory experimental validation	Demonstrated how transient storage buffering changes DC-bus droop and AC-side voltage behavior under source and load disturbances.	Lab-scale ratings, hybrid storage architecture, and disturbance profiles do not establish distribution-feeder hosting or field interoperability.	[30]
PV–storage electric-bus charging station	PV, BESS, and electric-bus charging with day-ahead scheduling under uncertainty; system-level 2026 study	Quantified coordinated PV–storage charging under uncertain renewable production and charging demand, reinforcing the need to couple storage scheduling to charging-service requirements.	The optimization objective, bus timetable, tariff assumptions, efficiency model, and station architecture determine the preferred schedule and limit direct feeder-to-feeder transfer.	[218]
MW-scale zinc–iron flow battery source–grid–load–storage control	1 MW-class flow-battery system model with SOC estimation and coordinated control; 2026 battery–grid study	Modeled battery SOC estimation, power allocation, and source–grid–load–storage coordination, showing that large-battery support depends on internal battery state and system loss.	Battery chemistry, control objectives, source/load profile, dispatch interval, and frequency-support context differ from PV-rich LV feeders and require revalidation before transfer.	[31]

The REVS observation counts also affect interpretation. Usable charger data covered 38/51 installations (74.5%), and discharge records covered 29/51 (56.9%). The remaining installations cannot be treated as zero-service devices or assumed available. Incomplete observation reduces confidence in fleet-wide extrapolation, and the report does not establish that missing records are random. The observed 0.146 MWh discharge relative to 18.4 MWh import (approximately 0.8%) supports a low-throughput interpretation for the specific contingency service but does not establish low wear under continuous regulation or daily energy shifting. No statistical correction is applied without the underlying dataset. REVS is therefore used as evidence of practical availability and implementation requirements rather than an estimate of universal V2G effectiveness [50].

The South Australian VPP result provides a complementary network observation: export capacity increased from 5 MW to 6–8 MW, equivalent to a calculated 20–60% increase, at 1000 sites over an 18-month trial. The report connects that result to dynamic operating

envelopes and local fallback [58]. It does not isolate an AI contribution or report net annual recovered PV energy under a common battery-aging model. These differences explain why numerical project results inform the synthesis without being pooled as equivalent performance effects.

The field evidence changes the interpretation of maturity. V2G should no longer be described simply as a simulation-stage concept, but pilot operation does not remove battery-life, customer-availability, standards, communications, or settlement constraints. Dynamic export limits likewise show that network-aware coordination can release additional renewable export capacity, but they require a trusted utility–aggregator interface and fail-safe local behavior. These functions have been demonstrated under specific technical and institutional conditions; they are not universally deployment ready. Broader implementation studies also show that coordinated EV-grid support depends on charger capability, feeder conditions, control architecture, and the interface between customer service and network objectives rather than transferring a controller diagram directly into field operation [56,80,147,219].

Nduka et al. [217] provide a PV–storage field comparator with power-quality measurements. Their network-wide 100% storage-uptake harmonic analysis is a desktop extrapolation informed by field data, not a measured full-penetration deployment: with other nonlinear loads, the modeled third-harmonic voltage reached 4.1094% against the study's 4.0% limit. The result illustrates why device-level conformity cannot substitute for feeder-level PQ assessment; it does not verify AI control or establish universal compliance margins.

6.4. Scope Limitations and Evidence Boundaries

Expert selection can omit relevant studies, and the supplementary title-query check cannot establish complete coverage. Its publication window and automated classification are distinct from the wider bibliography and claim-specific source appraisals. Heterogeneous feeders, battery duties, baselines, and assessment intervals prevent pooled effect estimates or universal control rankings. Field and laboratory findings remain conditional on the tested equipment, communication architecture, chemistry, and local connection rules. The broader AI–BESS reviews [21,22] provide complementary method coverage; the present synthesis concentrates on PQ constraints, battery duty, and source-attributed PV delivery.

7. Conclusions

PV utilization depends on the binding voltage, waveform, thermal, protection, or converter constraint. Battery services differ in their energy and current requirements: reactive and harmonic support consume converter headroom and can impose DC-side ripple, especially in single-phase or unbalanced operation, whereas sustained active support also requires usable energy and mobility reserve. Experimental ripple studies report different aging outcomes under different cells and duties [128,129]; a small mean energy exchange alone cannot establish negligible battery impact. AI should therefore be evaluated inside a verified electrical and battery feasibility layer.

Field projects establish that V2G and network-aware export control can operate outside simulation, subject to charger, communication, customer, and local-code constraints. None of the 30 selected sources in Supplementary Tables S1 and S5 demonstrates the combined field claim of AI coordination, independently assessed PQ compliance, battery-health limits, and long-duration net renewable-energy recovery. This combination remains a research gap within the assessed evidence. Comparisons should report PV-origin delivery at a declared balance point, grid charging and terminal energy separately, together with battery duty and compliance margin.

The quantitative evidence illustrates these boundaries: the South Australian trial expanded available export capacity from 5 MW to 6–8 MW, whereas REVS recorded only

0.146 MWh of discharge against 18.4 MWh imported; the two results characterize different services [50,58]. Cell-level shallow-cycle aging evidence also depends on the comparison with high-SOC storage [28]. These findings support conditional, service-specific conclusions rather than universal hosting or lifetime gains.

Future comparisons should evaluate controllers on the same feeder, battery model, converter limits, uncertainty set, and validation platform, using a common energy-attribution convention. This would distinguish decision-making gains from differences in physical assumptions.

Supplementary Materials: The following supporting information can be downloaded at https://www.mdpi.com/article/10.3390/batteries12110456/s1: Table S1: Principal sources assessed against system boundary, constraint treatment, reported outcome, and validation limit [19,24,27–29,35,43,50,58,127]; Table S2: Topic families used to frame the literature search; Table S3: Document types and citation-year groups of the 219 references cited in the current manuscript; Table S4: OpenAlex title queries executed on 2 October 2026 and occurrence counts before and after the publication-date restriction; Table S5: Additional sources used in the system, AI, and validation comparisons [17,20–22,25,26,30,31,40,48,49,56,106,124,131,171,174,201,217,218]. The accompanying files provide the retrieval log and record registers.

Author Contributions: Conceptualization, A.S.Z. and Y.H.; methodology, A.S.Z., H.J., Y.H. and A.M.G.; formal analysis, A.S.Z., H.J. and A.M.G.; investigation, A.S.Z., H.J. and A.M.G.; data curation, A.S.Z., H.J. and A.M.G.; visualization, A.S.Z. and A.M.G.; writing–original draft preparation, A.S.Z.; writing–review and editing, A.S.Z., H.J., Y.H., M.M., A.A.-S., A.M.G. and S.A.; supervision, Y.H., M.M. and A.A.-S.; project administration, A.S.Z. and S.A.; funding acquisition, S.A. All authors have read and agreed to the published version of the manuscript.

Funding: The Researchers would like to thank the Deanship of Graduate Studies and Scientific Research at Qassim University (https://www.qu.edu.sa) for financial support (QU-APC-2026).

Institutional Review Board Statement: Not applicable.

Informed Consent Statement: Not applicable.

Data Availability Statement: The source assessments, current bibliographic profile, and supplementary OpenAlex coverage check are provided in the Supplementary Material. Associated machine-readable files contain the retrieval log, deduplicated records, and automated classification outputs. The coverage check was executed on 2 October 2026; its reported comparison subset is restricted to publications dated through 30 June 2026. Underlying experimental and project data remain subject to the availability statements of their original sources.

Conflicts of Interest: The authors declare no conflicts of interest.

References

1. Vovos, P.; Kiprakis, A.; Wallace, A.; Harrison, G. Centralized and distributed voltage control: Impact on distributed generation penetration. *IEEE Trans. Power Syst.* **2007**, *22*, 476–483. [CrossRef]
2. Lin, C.; Hsieh, W.; Chen, C.; Hsu, C.; Ku, T. Optimization of photovoltaic penetration in distribution systems considering annual duration curve of solar irradiation. *IEEE Trans. Power Syst.* **2012**, *27*, 1090–1097. [CrossRef]
3. Oliveira, T.; Carvalho, P.; Ribeiro, P.; Bonatto, B. PV hosting capacity dependence on harmonic voltage distortion in low-voltage grids: Model validation with experimental data. *Energies* **2018**, *11*, 465. [CrossRef]
4. Chidurala, A.; Mithulananthan, N.; Saha, T.K. Harmonic impact of high penetration photovoltaic system on unbalanced distribution networks–learning from an urban photovoltaic network. *IET Renew. Power Gener.* **2016**, *10*, 485–494. [CrossRef]
5. Sakar, S.; Balci, M.; Abdel Aleem, S.; Zobaa, A. Increasing PV hosting capacity in distorted distribution systems using passive harmonic filtering. *Electr. Power Syst. Res.* **2017**, *148*, 74–86. [CrossRef]
6. Kabir, M.N.; Mishra, Y.; Ledwich, G.; Dong, Z.Y.; Wong, K.P. Coordinated Control of Grid-Connected Photovoltaic Reactive Power and Battery Energy Storage Systems to Improve the Voltage Profile of a Residential Distribution Feeder. *IEEE Trans. Ind. Inform.* **2014**, *10*, 967–977. [CrossRef]

7. Chukwu, U.; Mahajan, S. V2G parking lot with PV rooftop for capacity enhancement of a distribution system. *IEEE Trans. Sustain. Energy* **2014**, *5*, 119–127. [CrossRef]
8. Amamra, S.; Marco, J. Vehicle-to-grid aggregator to support power grid and reduce electric vehicle charging cost. *IEEE Access* **2019**, *7*, 178528–178538. [CrossRef]
9. Liu, X.; Aichhorn, A.; Liu, L.; Li, H. Coordinated control of distributed energy storage system with tap changer transformers for voltage rise mitigation under high photovoltaic penetration. *IEEE Trans. Smart Grid* **2012**, *3*, 897–906. [CrossRef]
10. Wang, Y.; Tan, K.; Peng, X.; So, P. Coordinated control of distributed energy-storage systems for voltage regulation in distribution networks. *IEEE Trans. Power Deliv.* **2016**, *31*, 1132–1141. [CrossRef]
11. Madani, S.S.; Shabeer, Y.; Fowler, M.; Panchal, S.; Chaoui, H.; Mekhilef, S.; Dou, S.X.; See, K. Artificial Intelligence and Digital Twin Technologies for Intelligent Lithium-Ion Battery Management Systems: A Comprehensive Review of State Estimation, Lifecycle Optimization, and Cloud-Edge Integration. *Batteries* **2025**, *11*, 298. [CrossRef]
12. Tong, Y.; Ma, H.; Du, F. Machine-Learning-Assisted Multi-Energy Coupling and Battery–Grid Coordination for Deep Decarbonization of Smart Integrated Energy Systems: Modeling, Optimization, and Applications. *Batteries* **2026**, *12*, 341. [CrossRef]
13. Al Qwaid, M.; Ramasamy, G.; Hossen, M.S. Physics-Informed Attention-Enhanced Reinforcement Learning for Safe and Explainable Fast Charging of Lithium-Ion Batteries. *Batteries* **2026**, *12*, 323. [CrossRef]
14. Bishla, S.; Khosla, A. Review of Power Quality and Stability of EV Charging with Grid and PV Solar. *Energy Technol.* **2024**, *12*, 2300744. [CrossRef]
15. Licari, J.; Rhaili, S.E.; Micallef, A.; Staines, C.S. Addressing voltage regulation challenges in low voltage distribution networks with high renewable energy and electrical vehicles: A critical review. *Energy Rep.* **2025**, *14*, 2977–2997. [CrossRef]
16. Ahmed, F.; Ahmad, S.; Rahman, M.T.; Hazari, M.R.; Faiz, R.; Ahmed, T.; Karimi, M. A holistic review of electric vehicle charging impacts on power distribution networks: Technical challenges, smart mitigation strategies and future directions. *Appl. Energy* **2026**, *402*, 126961. [CrossRef]
17. Dong, Q.; Song, X.; Gong, C.; Hu, C.; Rui, J.; Wang, T.; Xia, Z.; Wang, Z. Voltage Regulation Strategies in Photovoltaic-Energy Storage System Distribution Network: A Review. *Energies* **2025**, *18*, 2740. [CrossRef]
18. Atawi, I.E.; Al-Shetwi, A.Q.; Magableh, A.M.; Albalawi, O.H. Recent Advances in Hybrid Energy Storage System Integrated Renewable Power Generation: Configuration, Control, Applications, and Future Directions. *Batteries* **2023**, *9*, 29. [CrossRef]
19. Yin, K.; Xiao, Y.; Shen, X.; Zhu, Y.; Yang, Y. Review of Photovoltaic–Battery Energy Storage Systems for Grid-Forming Operation. *Batteries* **2024**, *10*, 288. [CrossRef]
20. Coccato, S.; Barhmi, K.; Lampropoulos, I.; Golroodbari, S.; van Sark, W. A Review of Battery Energy Storage Optimization in the Built Environment. *Batteries* **2025**, *11*, 179. [CrossRef]
21. Ketjoy, N.; Muna, Y.B.; Kaewpanha, M.; Chamsa-ard, W.; Suriwong, T.; Termritthikun, C. Grid-Scale Battery Energy Storage and AI-Driven Intelligent Optimization for Techno-Economic and Environmental Benefits: A Systematic Review. *Batteries* **2026**, *12*, 31. [CrossRef]
22. Benbouhenni, H.; Bizon, N. Artificial Intelligence-Enabled Battery Energy Storage Systems for Renewable Energy: A Comprehensive Review of Technologies, Applications, Challenges, and Future Directions. *Batteries* **2026**, *12*, 353. [CrossRef]
23. Lehtola, T. Vehicle-to-grid applications and battery cycle aging: A review. *Renew. Sustain. Energy Rev.* **2025**, *208*, 115013. [CrossRef]
24. Pinoski, L.; Latos, B.; Marigny, D.; Jensen, T.; De Los Reyes, A.; Helwig, B.; Menezes, P.L. Rechargeable Batteries for Grid-Scale Energy Storage: Technologies, Performance, and Emerging Directions. *Batteries* **2026**, *12*, 264. [CrossRef]
25. Filip, R.; Püvi, V.; Paar, M.; Lehtonen, M. Analyzing the Impact of EV and BESS Deployment on PV Hosting Capacity of Distribution Networks. *Energies* **2022**, *15*, 7921. [CrossRef]
26. Khunkitti, S.; Pompern, N.; Premrudeepreechacharn, S.; Siritaratiwat, A. Optimal Placement and Capacity of BESS and PV in EV Integrated Distribution Systems: The Tenth Feeder of Phitsanulok Substation Case Study. *Batteries* **2024**, *10*, 212. [CrossRef]
27. Gao, Y.; Yu, N. Model-augmented safe reinforcement learning for Volt-VAR control in power distribution networks. *Appl. Energy* **2022**, *313*, 118762. [CrossRef]
28. Darikas, G.; Kirca, M.C.; Saniee, N.F.; Rashid, M.; Muhaddisoglu, I.M.; Dinh, T.Q.; McGordon, A. Experimental Investigation of the Impact of V2G Cycling on the Lifetime of Lithium-Ion Cells Based on Real-World Usage Data. *Batteries* **2026**, *12*, 22. [CrossRef]
29. Akinwola, A.B.; Alkuhayli, A. Physics-Informed Neural Network-Based Intelligent Control for Photovoltaic Charge Allocation in Multi-Battery Energy Systems. *Batteries* **2026**, *12*, 46. [CrossRef]
30. Asrari, A.; Pandey, A.; LaMarche, C.E.; Kowalski, R.P. From Renewable Variability to Hybrid Stability: Analytical and Experimental Insights into a Transient Buffering Battery–Supercapacitor Framework in a Lab-Scale PV–Wind Microgrid. *Batteries* **2026**, *12*, 157. [CrossRef]
31. Wang, S.; Kong, L.; Leung, P.; Fang, S.; Yang, K.; Fan, X. Collaborative Control Strategy of Megawatt-Level Zinc–Iron Flow Battery Energy Storage System Based on Source–Grid–Load–Storage Integration. *Batteries* **2026**, *12*, 139. [CrossRef]

32. *IEEE Std 519-2022 (Revision of IEEE Std 519-2014)*; IEEE Standard for Harmonic Control in Electric Power Systems. Institute of Electrical and Electronics Engineers: New York, NY, USA, 2022. [CrossRef]
33. Rodríguez-Pajarón, P.; Hernández, A.; Milanović, J. Probabilistic assessment of the impact of electric vehicles and nonlinear loads on power quality in residential networks. *Int. J. Electr. Power Energy Syst.* **2021**, *129*, 106807. [CrossRef]
34. Kebede, A.; Kalogiannis, T.; Berecibar, M.; Van Mierlo, J. A comprehensive review of stationary energy storage devices for large scale renewable energy sources grid integration. *Renew. Sustain. Energy Rev.* **2022**, *159*, 112213. [CrossRef]
35. Chen, Y.; Liu, X.; Fu, Y. State-of-Health Predictive Energy Management and Grid-Forming Control for Battery Energy Storage Systems. *Batteries* **2026**, *12*, 15. [CrossRef]
36. Drude, L.; Pereira Junior, L.; Rüther, R. Photovoltaics (PV) and electric vehicle-to-grid (V2G) strategies for peak demand reduction in urban regions in Brazil in a smart grid environment. *Renew. Energy* **2014**, *68*, 443–451. [CrossRef]
37. Sagaria, S.; van der Kam, M.; Boström, T. Vehicle-to-grid impact on battery degradation and estimation of V2G economic compensation. *Appl. Energy* **2025**, *377*, 124546. [CrossRef]
38. Rafi, F.; Hossain, M.; Lu, J. Hierarchical controls selection based on PV penetrations for voltage rise mitigation in a LV distribution network. *Int. J. Electr. Power Energy Syst.* **2016**, *81*, 123–139. [CrossRef]
39. Hu, J.; Ye, C.; Ding, Y.; Tang, J.; Liu, S. A distributed MPC to exploit reactive power V2G for real-time voltage regulation in distribution networks. *IEEE Trans. Smart Grid* **2022**, *13*, 576–588. [CrossRef]
40. Nguyen, H.; Hosani, K.; Al-Sumaiti, A.; Nguyen, T.; Jaafari, K.; Alsawalhi, J.; El Moursi, M. Fast harmonic rejecting control design to enable active support of charging stations to micro-grids under distortion. *IEEE Trans. Transp. Electrif.* **2023**, *9*, 4132–4146. [CrossRef]
41. Hou, Q.; Dai, N.; Huang, Y. Voltage Regulation Enhanced Hierarchical Coordinated Volt/Var and Volt/Watt Control for Active Distribution Networks with Soft Open Points. *IEEE Trans. Sustain. Energy* **2024**, *15*, 2021–2037. [CrossRef]
42. Kim, D.J.; Kim, B.; Yoon, C.; Nguyen, N.D.; Lee, Y.I. Disturbance Observer-Based Model Predictive Voltage Control for Electric-Vehicle Charging Station in Distribution Networks. *IEEE Trans. Smart Grid* **2023**, *14*, 545–558. [CrossRef]
43. Ding, Y.; Chen, X.; Wang, J. Deep Reinforcement Learning-Based Method for Joint Optimization of Mobile Energy Storage Systems and Power Grid with High Renewable Energy Sources. *Batteries* **2023**, *9*, 219. [CrossRef]
44. Patra, S.; Kishor, N.; Mohanty, S.R.; Ray, P.K. Power quality assessment in 3-phase grid connected PV system with single and dual stage circuits. *Int. J. Electr. Power Energy Syst.* **2016**, *75*, 275–288. [CrossRef]
45. Solatialkaran, D.; Zare, F.; Saha, T.K.; Sharma, R. A novel approach in filter design for grid-connected inverters used in renewable energy systems. *IEEE Trans. Sustain. Energy* **2020**, *11*, 154–164. [CrossRef]
46. Caro, L.; Ramos, G.; Rauma, K.; Rodriguez, D.; Martinez, D.; Rehtanz, C. State of charge influence on the harmonic distortion from electric vehicle charging. *IEEE Trans. Ind. Appl.* **2021**, *57*, 2077–2088. [CrossRef]
47. Kampker, A.; Spath, B.; Song, X.; Wang, D. Modelling of Battery Energy Storage Systems Under Real-World Applications and Conditions. *Batteries* **2025**, *11*, 392. [CrossRef]
48. Yong, J.; Fazeli, S.; Ramachandaramurthy, V.; Tan, K. Design and development of a three-phase off-board electric vehicle charger prototype for power grid voltage regulation. *Energy* **2017**, *133*, 128–141. [CrossRef]
49. Mather, B. *NREL/SCE High-Penetration PV Integration Project: Report on Field Demonstration of Advanced Inverter Functionality in Fontana, California*; Technical Report NREL/TP-5D00-62483; National Renewable Energy Laboratory: Golden, CO, USA, 2014.
50. Australian Renewable Energy Agency. *Insights from the Realising Electric Vehicle-to-Grid Services (REVS) Trial*; Technical Report; Australian Renewable Energy Agency: Canberra, Australia, 2024.
51. *IEEE Std 1547-2018 (Revision of IEEE Std 1547-2003);* IEEE Standard for Interconnection and Interoperability of Distributed Energy Resources with Associated Electric Power Systems Interfaces. Institute of Electrical and Electronics Engineers: New York, NY, USA, 2018. [CrossRef]
52. *IEC 61000-4-30:2025*; Electromagnetic Compatibility (EMC)—Part 4-30: Testing and Measurement Techniques—Power Quality Measurement Methods, 4th ed. International Electrotechnical Commission: Geneva, Switzerland, 2025.
53. *IEC 61000-4-7:2002+AMD1:2008 CSV*; Electromagnetic Compatibility (EMC)—Part 4-7: Testing and Measurement Techniques—General Guide on Harmonics and Interharmonics Measurements and Instrumentation, for Power Supply Systems and Equipment Connected Thereto. Consolidated Version, Edition 2.1. International Electrotechnical Commission: Geneva, Switzerland, 2009.
54. *EN 50160:2022+A1:2025*; Voltage Characteristics of Electricity Supplied by Public Electricity Networks. European Committee for Electrotechnical Standardization (CENELEC): Brussels, Belgium, 2025.
55. Tiburtini, F.M.; Lo Franco, F.; Ricco, M. Multi-Objective Sizing Method for PV-BESS Integration with EV Charging Stations and Analysis Across Different Parking Scenarios. *Batteries* **2025**, *11*, 422. [CrossRef]
56. Marra, F.; Yang, G.; Traeholt, C.; Larsen, E.; Ostergaard, J.; Blazic, B.; Deprez, W. EV charging facilities and their application in LV feeders with photovoltaics. *IEEE Trans. Smart Grid* **2013**, *4*, 1533–1540. [CrossRef]
57. Van Roy, J.; Leemput, N.; Geth, F.; Salenbien, R.; Buscher, J.; Driesen, J. Apartment building electricity system impact of operational electric vehicle charging strategies. *IEEE Trans. Sustain. Energy* **2014**, *5*, 264–272. [CrossRef]

58. SA Power Networks. *Advanced VPP Grid Integration: Final Report*; Technical Report; SA Power Networks: Keswick, Australia, 2021.
59. Omran, W.; Kazerani, M.; Salama, M. A clustering-based method for quantifying the effects of large on-grid PV systems. *IEEE Trans. Power Deliv.* **2010**, *25*, 2617–2625. [CrossRef]
60. Emmanuel, M.; Rayudu, R. The impact of single-phase grid-connected distributed photovoltaic systems on the distribution network using P-Q and P-V models. *Int. J. Electr. Power Energy Syst.* **2017**, *91*, 20–33. [CrossRef]
61. Li, C.; Yang, Y.; Cao, Y.; Wang, L.; Blaabjerg, F. Frequency and voltage stability analysis of grid-forming virtual synchronous generator attached to weak grid. *IEEE J. Emerg. Sel. Top. Power Electron.* **2022**, *10*, 2662–2671. [CrossRef]
62. Shintai, T.; Miura, Y.; Ise, T. Oscillation damping of a distributed generator using a virtual synchronous generator. *IEEE Trans. Power Deliv.* **2014**, *29*, 668–676. [CrossRef]
63. Heydari, E.; Varjani, A.; Diallo, D. A dual-function power decoupling circuit for single-stage grid-connected PV inverter. *IEEE Trans. Power Electron.* **2022**, *37*, 7422–7431. [CrossRef]
64. Olivier, F.; Aristidou, P.; Ernst, D.; Van Cutsem, T. Active management of low-voltage networks for mitigating overvoltages due to photovoltaic units. *IEEE Trans. Smart Grid* **2016**, *7*, 926–936. [CrossRef]
65. Weckx, S.; Driesen, J. Optimal local reactive power control by PV inverters. *IEEE Trans. Sustain. Energy* **2016**, *7*, 1624–1633. [CrossRef]
66. Li, P.; Gu, W.; Long, H.; Cao, G.; Cao, Z.; Xu, B.; Pan, J. High-precision dynamic modeling of two-staged photovoltaic power station clusters. *IEEE Trans. Power Syst.* **2019**, *34*, 4393–4407. [CrossRef]
67. Li, P.; Gu, W.; Wang, L.; Xu, B.; Wu, M.; Shen, W. Dynamic equivalent modeling of two-staged photovoltaic power station clusters based on dynamic affinity propagation clustering algorithm. *Int. J. Electr. Power Energy Syst.* **2018**, *95*, 463–475. [CrossRef]
68. Li, P. Accurate Modeling and Simulation Algorithm of Distribution Network with High-Penetration Distributed Photovoltaic. Ph.D. Thesis, Southeast University, Nanjing, China, 2020. [CrossRef]
69. Ansari, B.; Simoes, M. Distributed energy management of PV-storage systems for voltage rise mitigation. *Technol. Econ. Smart Grids Sustain. Energy* **2017**, *2*, 15. [CrossRef]
70. Tonkoski, R.; Lopes, L.; El-Fouly, T. Coordinated active power curtailment of grid connected PV inverters for overvoltage prevention. *IEEE Trans. Sustain. Energy* **2011**, *2*, 139–147. [CrossRef]
71. Farhoodnea, M.; Mohamed, A.; Shareef, H.; Zayandehroodi, H. An enhanced method for contribution assessment of utility and customer harmonic distortions in radial and weakly meshed distribution systems. *Int. J. Electr. Power Energy Syst.* **2012**, *43*, 222–229. [CrossRef]
72. Qian, K.; Zhou, C.; Allan, M.; Yuan, Y. Modeling of load demand due to EV battery charging in distribution systems. *IEEE Trans. Power Syst.* **2011**, *26*, 802–810. [CrossRef]
73. Masoum, A.; Deilami, S.; Moses, P.; Masoum, M.; Abu-Siada, A. Smart load management of plug-in electric vehicles in distribution and residential networks with charging stations for peak shaving and loss minimization considering voltage regulation. *IET Gener. Transm. Distrib.* **2011**, *5*, 877. [CrossRef]
74. Gao, C.; Zhang, L. A survey of influence of electric vehicle charging on power grid. *Power Syst. Technol.* **2011**, *35*, 127–131. [CrossRef]
75. Van Roy, J.; Leemput, N.; Geth, F.; Buscher, J.; Salenbien, R.; Driesen, J. Electric vehicle charging in an office building microgrid with distributed energy resources. *IEEE Trans. Sustain. Energy* **2014**, *5*, 1389–1396. [CrossRef]
76. Gomez, J.; Morcos, M. Impact of EV Battery Chargers on the Power Quality of Distribution Systems. *IEEE Power Eng. Rev.* **2002**, *22*, 63. [CrossRef]
77. Jiang, C.; Torquato, R.; Salles, D.; Xu, W. Method to assess the power-quality impact of plug-in electric vehicles. *IEEE Trans. Power Deliv.* **2014**, *29*, 958–965. [CrossRef]
78. Nworgu, O.A.; Chukwu, U.C.; Okezie, C.G.; Chukwu, N.B. Economic prospects and market operations of V2G in electric distribution network. In Proceedings of the IEEE PES Transmission and Distribution Conference and Exposition (T&D), Dallas, TX, USA, 2–5 May 2016; pp. 1–5. [CrossRef]
79. Yu, R.; Zhong, W.; Xie, S.; Yuen, C.; Gjessing, S.; Zhang, Y. Balancing power demand through EV mobility in vehicle-to-grid mobile energy networks. *IEEE Trans. Ind. Inform.* **2016**, *12*, 79–90. [CrossRef]
80. Azzouz, M.; Shaaban, M.; El-Saadany, E. Real-time optimal voltage regulation for distribution networks incorporating high penetration of pevs. *IEEE Trans. Power Syst.* **2015**, *30*, 3234–3245. [CrossRef]
81. Li, Y.; Li, L.; Peng, C.; Zou, J. An MPC-Based Optimized Control Approach for EV-Based Voltage Regulation in Distribution Grid. *Electr. Power Syst. Res.* **2019**, *172*, 152–160. [CrossRef]
82. Li, H.; Azzouz, M.; Hamad, A. Cooperative voltage control in MV distribution networks with electric vehicle charging stations and photovoltaic dgs. *IEEE Syst. J.* **2021**, *15*, 2989–3000. [CrossRef]
83. Wang, Y.; John, T.; Xiong, B. A two-level coordinated voltage control scheme of electric vehicle chargers in low-voltage distribution networks. *Electr. Power Syst. Res.* **2019**, *168*, 218–227. [CrossRef]

84. Wang, X.; He, Z.; Yang, J. Unified strategy for electric vehicles participate in voltage and frequency regulation with active power in city grid. *IET Gener. Transm. Distrib.* **2019**, *13*, 3281–3291. [CrossRef]
85. Voronin, V.; Nepsha, F.; Ilyushin, P. Determining Volt/Var Characteristics of Electric Vehicle Charging Station Inverters for Voltage Regulation in Distribution Networks. *World Electr. Veh. J.* **2024**, *15*, 553. [CrossRef]
86. Ahmadi, A.; Tavakoli, A.; Jamborsalamati, P.; Rezaei, N.; Miveh, M.R.; Gandoman, F.H.; Heidari, A.; Nezhad, A.A.E. Power quality improvement in smart grids using electric vehicles: A review. *IET Electr. Syst. Transp.* **2019**, *9*, 53–64. [CrossRef]
87. Yilmaz, M.; Krein, P. Review of the Impact of Vehicle-to-Grid Technologies on Distribution Systems and Utility Interfaces. *IEEE Trans. Power Electron.* **2013**, *28*, 5673–5689. [CrossRef]
88. Hu, Z.; Song, Y.; Xu, Z. Impacts and utilization of electric vehicles integration into power systems. *Proc. CSEE* **2012**, *32*, 1–10. [CrossRef]
89. Cai, L.; Shang, B.; Gao, L.; Dai, N.; Xu, Q.; Wang, K.; Zhang, Y.; Xu, K. Review of Research and Application on Orderly Charging of Electric Vehicles. *South. Power Syst. Technol.* **2023**, *17*, 97–107. [CrossRef]
90. Tian, L.; Zhang, M.; Wang, H. Evaluation and solutions for electric vehicles' impact on the grid. *Proc. CSEE* **2012**, *32*, 43–49. [CrossRef]
91. Singh, B.; Dubey, P.K. Distributed power generation planning for distribution networks using electric vehicles: Systematic attention to challenges and opportunities. *J. Energy Storage* **2022**, *48*, 104030. [CrossRef]
92. Liu, S.; Zhou, B.; Peng, Z. Reconfiguration of distribution network with distributed generations and electric vehicles using multi-agent. *Proc. CSU-EPSA* **2017**, *29*, 91–97. [CrossRef]
93. Yang, S.; Luan, Z.; Qin, Z. Research of Charging(Discharging) Orderly and Optimizing Load Curve for Electric Vehicles Based on Dynamic Electric Price and V2G. In Proceedings of the 2016 Asia Conference on Power and Electrical Engineering (ACPEE 2016), Bangkok, Thailand, 20–22 March 2016; MATEC Web of Conferences; Volume 55, p. 06006. [CrossRef]
94. Aluisio, B.; Conserva, A.; Dicorato, M.; Forte, G.; Trovato, M. Optimal operation planning of V2G-equipped microgrid in the presence of EV aggregator. *Electr. Power Syst. Res.* **2017**, *152*, 295–305. [CrossRef]
95. Tabatabaee, S.; Mortazavi, S.; Niknam, T. Stochastic scheduling of local distribution systems considering high penetration of plug-in electric vehicles and renewable energy sources. *Energy* **2017**, *121*, 480–490. [CrossRef]
96. Zhong, J.; He, L.; Li, C.; Cao, Y.; Wang, J.; Fang, B.; Zeng, L.; Xiao, G. Coordinated control for large-scale EV charging facilities and energy storage devices participating in frequency regulation. *Appl. Energy* **2014**, *123*, 253–262. [CrossRef]
97. Jia, L.; Hu, Z.; Song, Y. Joint planning of distribution networks with distributed energy storage systems and EV stations. *Proc. CSEE* **2017**, *37*, 73–84. [CrossRef]
98. Fathabadi, H. Novel solar powered electric vehicle charging station with the capability of vehicle-to-grid. *Sol. Energy* **2017**, *142*, 136–143. [CrossRef]
99. Lih, W.C.; Yen, J.H.; Shieh, F.H.; Liao, Y.M. Second Use of Retired Lithium-ion Battery Packs from Electric Vehicles: Technological Challenges, Cost Analysis and Optimal Business Model. In Proceedings of the International Symposium on Computer, Consumer and Control (IS3C), Taichung, Taiwan, 4–6 June 2012; pp. 381–384. [CrossRef]
100. Faria, R.; Marques, P.; Garcia, R.; Moura, P.; Freire, F.; Delgado, J.; de Almeida, A.T. Primary and secondary use of electric mobility batteries from a life cycle perspective. *J. Power Sources* **2014**, *262*, 169–177. [CrossRef]
101. Brauer, S.; Monhof, M.; Klor, B.; Plenter, F.; Beverungen, D.; Siemen, C. Residential Energy Storage from Repurposed Electric Vehicle Batteries: Market Overview and Development of a Service-Centered Business Model. In Proceedings of the IEEE International Conference on Business Informatics (CBI), Paris, France, 29 August–1 September 2016; pp. 143–152. [CrossRef]
102. Li, Y.; Davis, C.; Lukszo, Z.; Weijnen, M. Electric vehicle charging in China's power system: Energy, economic and environmental trade-offs and policy implications. *Appl. Energy* **2016**, *173*, 535–554. [CrossRef]
103. Zakariazadeh, A.; Jadid, S.; Siano, P. Multi-objective scheduling of electric vehicles in smart distribution system. *Energy Convers. Manag.* **2014**, *79*, 43–53. [CrossRef]
104. Zhao, Y.; Noori, M.; Tatari, O. Vehicle to Grid regulation services of electric delivery trucks: Economic and environmental benefit analysis. *Appl. Energy* **2016**, *170*, 161–175. [CrossRef]
105. Lu, X.; Zhou, K.; Yang, S. Multi-objective optimal dispatch of microgrid containing electric vehicles. *J. Clean. Prod.* **2017**, *165*, 1572–1581. [CrossRef]
106. Cenex. *Project Sciurus Trial Insights: Findings from 300 Domestic Vehicle-to-Grid Units in 2020*; Technical Report; Cenex: Loughborough, UK, 2021.
107. Mitali, J.; Dhinakaran, S.; Mohamad, A. Energy storage systems: A review. *Energy Storage Sav.* **2022**, *1*, 166–216. [CrossRef]
108. Bullich-Massague, E.; Cifuentes-Garcia, F.J.; Glenny-Crende, I.; Cheah-Mane, M.; Aragues-Penalba, M.; Diaz-Gonzalez, F.; Gomis-Bellmunt, O. A review of energy storage technologies for large scale photovoltaic power plants. *Appl. Energy* **2020**, *274*, 115213. [CrossRef]
109. Luo, X.; Wang, J.; Dooner, M.; Clarke, J. Overview of current development in electrical energy storage technologies and the application potential in power system operation. *Appl. Energy* **2015**, *137*, 511–536. [CrossRef]

110. Johnston, L.; Diaz-Gonzalez, F.; Gomis-Bellmunt, O.; Corchero-Garcia, C.; Cruz-Zambrano, M. Methodology for the economic optimisation of energy storage systems for frequency support in wind power plants. *Appl. Energy* **2015**, *137*, 660–669. [CrossRef]
111. Zhou, S.; Han, Y.; Chen, S.; Yang, P.; Mahmoud, K.; Darwish, M.M.; Matti, L.; Zalhaf, A.S. A multiple uncertainty-based Bi-level expansion planning paradigm for distribution networks complying with energy storage system functionalities. *Energy* **2023**, *275*, 127511. [CrossRef]
112. Zhang, B.; Lam, A.; Dominguez-Garcia, A.; Tse, D. An optimal and distributed method for voltage regulation in power distribution systems. *IEEE Trans. Power Syst.* **2015**, *30*, 1714–1726. [CrossRef]
113. Lim, K.; Lim, Y.; Wong, J.; Chua, K. Distributed Energy Storage with Real and Reactive Power Controller for Power Quality Issues Caused by Renewable Energy and Electric Vehicles. *J. Energy Eng.* **2016**, *142*, 04015051. [CrossRef]
114. Chellaswamy, C.; Ramesh, R. Future renewable energy option for recharging full electric vehicles. *Renew. Sustain. Energy Rev.* **2017**, *76*, 824–838. [CrossRef]
115. Hannan, M.; Hoque, M.; Mohamed, A.; Ayob, A. Review of energy storage systems for electric vehicle applications: Issues and challenges. *Renew. Sustain. Energy Rev.* **2017**, *69*, 771–789. [CrossRef]
116. Das, H.; Rahman, M.; Li, S.; Tan, C. Electric vehicles standards, charging infrastructure, and impact on grid integration: A technological review. *Renew. Sustain. Energy Rev.* **2020**, *120*, 109618. [CrossRef]
117. Tan, K.; Ramachandaramurthy, V.; Yong, J. Integration of electric vehicles in smart grid: A review on vehicle to grid technologies and optimization techniques. *Renew. Sustain. Energy Rev.* **2016**, *53*, 720–732. [CrossRef]
118. Romo, R.; Micheloud, O. Power quality of actual grids with plug-in electric vehicles in presence of renewables and micro-grids. *Renew. Sustain. Energy Rev.* **2015**, *46*, 189–200. [CrossRef]
119. Shah, R.; Mithulananthan, N.; Bansal, R.; Ramachandaramurthy, V. A review of key power system stability challenges for large-scale PV integration. *Renew. Sustain. Energy Rev.* **2015**, *41*, 1423–1436. [CrossRef]
120. Nema, P.; Nema, R.; Rangnekar, S. A current and future state of art development of hybrid energy system using wind and PV-solar: A review. *Renew. Sustain. Energy Rev.* **2009**, *13*, 2096–2103. [CrossRef]
121. Aneke, M.; Wang, M. Energy storage technologies and real life applications – a state of the art review. *Appl. Energy* **2016**, *179*, 350–377. [CrossRef]
122. Vazquez, S.; Lukic, S.M.; Galvan, E.; Franquelo, L.G.; Carrasco, J.M. Energy storage systems for transport and grid applications. *IEEE Trans. Ind. Electron.* **2010**, *57*, 3881–3895. [CrossRef]
123. Diaz-Gonzalez, F.; Sumper, A.; Gomis-Bellmunt, O.; Villafafila-Robles, R. A review of energy storage technologies for wind power applications. *Renew. Sustain. Energy Rev.* **2012**, *16*, 2154–2171. [CrossRef]
124. de Oliveira, J.F.L.; de Mattos Neto, P.S.G.; Siqueira, H.V.; Santos, D.S.d.O., Jr.; Lima, A.R.; Madeiro, F.; Dantas, D.A.P.; Cavalcanti, M.d.M.; Pereira, A.C.; Marinho, M.H.N. Forecasting Methods for Photovoltaic Energy in the Scenario of Battery Energy Storage Systems: A Comprehensive Review. *Energies* **2023**, *16*, 6638. [CrossRef]
125. Li, X.; Hui, D.; Lai, X. Battery Energy Storage Station (BESS)-Based Smoothing Control of Photovoltaic (PV) and Wind Power Generation Fluctuations. *IEEE Trans. Sustain. Energy* **2013**, *4*, 464–473. [CrossRef]
126. Bhayo, B.A.; Al-Kayiem, H.H.; Gilani, S.I.; Ismail, F.B. Power management optimization of hybrid solar photovoltaic-battery integrated with pumped-hydro-storage system for standalone electricity generation. *Energy Convers. Manag.* **2020**, *215*, 112942. [CrossRef]
127. Dubarry, M.; Devie, A.; McKenzie, K. Durability and reliability of electric vehicle batteries under electric utility grid operations: Bidirectional charging impact analysis. *J. Power Sources* **2017**, *358*, 39–49. [CrossRef]
128. Uddin, K.; Moore, A.D.; Barai, A.; Marco, J. The effects of high frequency current ripple on electric vehicle battery performance. *Appl. Energy* **2016**, *178*, 142–154. [CrossRef]
129. Bessman, A.; Soares, R.; Wallmark, O.; Svens, P.; Lindbergh, G. Aging effects of AC harmonics on lithium-ion cells. *J. Energy Storage* **2019**, *21*, 741–749. [CrossRef]
130. Bala, S.; Tengnér, T.; Rosenfeld, P.; Delince, F. The effect of low frequency current ripple on the performance of a Lithium Iron Phosphate (LFP) battery energy storage system. In Proceedings of the 2012 IEEE Energy Conversion Congress and Exposition, Raleigh, NC, USA, 15–20 September 2012; pp. 3485–3492. [CrossRef]
131. Kou, P.; Liang, D.; Wang, C.; Wu, Z.; Gao, L. Safe deep reinforcement learning-based constrained optimal control scheme for active distribution networks. *Appl. Energy* **2020**, *264*, 114772. [CrossRef]
132. Dalal, G.; Dvijotham, K.; Vecerik, M.; Hester, T.; Paduraru, C.; Tassa, Y. Safe Exploration in Continuous Action Spaces. *arXiv* **2018**, arXiv:1801.08757.
133. Achiam, J.; Held, D.; Tamar, A.; Abbeel, P. Constrained Policy Optimization. In Proceedings of the 34th International Conference on Machine Learning, Sydney, Australia, 6–11 August 2017; Volume 70, pp. 22–31.
134. Lucas, A.; Bonavitacola, F.; Kotsakis, E.; Fulli, G. Grid harmonic impact of multiple electric vehicle fast charging. *Electr. Power Syst. Res.* **2015**, *127*, 13–21. [CrossRef]

135. Raval, D.Y.; Pandya, S.N. Phase shifting strategy for mitigation of local voltage rise in highly PV penetrated distribution network. In Proceedings of the IEEE International Conference on Power Systems (ICPS), Kharagpur, India, 16–18 December 2021; pp. 1–6. [CrossRef]
136. Patil, A.; Girgaonkar, R.; Musunuri, S.K. Impacts of increasing photovoltaic penetration on distribution grid - voltage rise case study. In Proceedings of the International Conference on Advances in Green Energy (ICAGE), Thiruvananthapuram, India, 17–18 December 2014; pp. 100–105. [CrossRef]
137. Hasheminamin, M.; Agelidis, V.; Salehi, V.; Teodorescu, R.; Hredzak, B. Index-based assessment of voltage rise and reverse power flow phenomena in a distribution feeder under high PV penetration. *IEEE J. Photovolt.* **2015**, *5*, 1158–1168. [CrossRef]
138. Aziz, T.; Ketjoy, N. PV penetration limits in low voltage networks and voltage variations. *IEEE Access* **2017**, *5*, 16784–16792. [CrossRef]
139. Weckx, S.; Gonzalez, C.; Driesen, J. Combined central and local active and reactive power control of PV inverters. *IEEE Trans. Sustain. Energy* **2014**, *5*, 776–784. [CrossRef]
140. Antoniadou-Plytaria, K.; Kouveliotis-Lysikatos, I.; Georgilakis, P.; Hatziargyriou, N. Distributed and decentralized voltage control of smart distribution networks: Models, methods, and future research. *IEEE Trans. Smart Grid* **2017**, *8*, 2999–3008. [CrossRef]
141. Samadi, A.; Eriksson, R.; Soder, L.; Rawn, B.; Boemer, J. Coordinated active power-dependent voltage regulation in distribution grids with PV systems. *IEEE Trans. Power Deliv.* **2014**, *29*, 1454–1464. [CrossRef]
142. Wang, Y.; Zhang, P.; Li, W.; Xiao, W.; Abdollahi, A. Online overvoltage prevention control of photovoltaic generators in microgrids. *IEEE Trans. Smart Grid* **2012**, *3*, 2071–2078. [CrossRef]
143. Ghosh, S.; Rahman, S.; Pipattanasomporn, M. Distribution voltage regulation through active power curtailment with PV inverters and solar generation forecasts. *IEEE Trans. Sustain. Energy* **2017**, *8*, 13–22. [CrossRef]
144. Hashemi, S.; Østergaard, J. Methods and strategies for overvoltage prevention in low voltage distribution systems with PV. *IET Renew. Power Gener.* **2017**, *11*, 205–214. [CrossRef]
145. *IEC 61000-4-15:2010*; Electromagnetic Compatibility (EMC)—Part 4-15: Testing and Measurement Techniques—Flickermeter—Functional and Design Specifications. Edition 2.0; Corrigendum 1 published 2012; International Electrotechnical Commission: Geneva, Switzerland, 2010.
146. Baptista, J.E.R.; Rodrigues, A.B.; da Silva, M.G. Probabilistic analysis of PV generation impacts on voltage sags in LV distribution networks considering failure rates dependent on feeder loading. *IEEE Trans. Sustain. Energy* **2019**, *10*, 1342–1350. [CrossRef]
147. Foster, J.; Trevino, G.; Kuss, M.; Caramanis, M. Plug-in electric vehicle and voltage support for distributed solar: Theory and application. *IEEE Syst. J.* **2013**, *7*, 881–888. [CrossRef]
148. Niitsoo, J.; Taklaja, P.; Palu, I.; Klüss, J. Power quality issues concerning photovoltaic generation and electrical vehicle loads in distribution grids. *Smart Grid Renew. Energy* **2015**, *6*, 164–177. [CrossRef]
149. Pinto, R.; Mariano, S.; Calado, M.; de Souza, J. Impact of rural grid-connected photovoltaic generation systems on power quality. *Energies* **2016**, *9*, 739. [CrossRef]
150. Naderipour, A.; Abdul-Malek, Z.; Miveh, M.R.; Moghaddam, M.J.H.; Kalam, A.; Gandoman, F.H. A harmonic compensation strategy in a grid-connected photovoltaic system using zero-sequence control. *Energies* **2018**, *11*, 2629. [CrossRef]
151. Hu, Z.; Han, Y.; Zalhaf, A.; Zhou, S.; Zhao, E.; Yang, P. Harmonic sources modeling and characterization in modern power systems: A comprehensive overview. *Electr. Power Syst. Res.* **2023**, *218*, 109234. [CrossRef]
152. Burch, R.; Chang, G.; Hatziadoniu, C.; Grady, M.; Liu, Y.; Marz, M.; Ortmeyer, T.; Ranade, S.; Ribeiro, P.; Xu, W. Impact of aggregate linear load modeling on harmonic analysis: A comparison of common practice and analytical models. *IEEE Trans. Power Deliv.* **2003**, *18*, 625–630. [CrossRef]
153. Kalair, A.; Abas, N.; Kalair, A.; Saleem, Z.; Khan, N. Review of harmonic analysis, modeling and mitigation techniques. *Renew. Sustain. Energy Rev.* **2017**, *78*, 1152–1187. [CrossRef]
154. Dai, J.; Shokooh, F. Industrial and commercial power system harmonic studies: Introduction to IEEE Std. 3002.8-2018. In Proceedings of the IEEE Industrial and Commercial Power Systems Technical Conference (ICPS), Victoria, BC, Canada, 10–13 May 2021; pp. 1–11. [CrossRef]
155. Munir, S.; Li, Y. Residential distribution system harmonic compensation using PV interfacing inverter. *IEEE Trans. Smart Grid* **2013**, *4*, 816–827. [CrossRef]
156. Hengsritawat, V.; Tayjasanant, T.; Nimpitiwan, N. Optimal sizing of photovoltaic distributed generators in a distribution system with consideration of solar radiation and harmonic distortion. *Int. J. Electr. Power Energy Syst.* **2012**, *39*, 36–47. [CrossRef]
157. Farooq, H.; Zhou, C.; Farrag, M. Analyzing the harmonic distortion in a distribution system caused by the non-linear residential loads. *SGCE* **2013**, *2*, 46–51. [CrossRef]
158. Deihimi, A.; Rahmani, A. Application of echo state networks for estimating voltage harmonic waveforms in power systems considering a photovoltaic system. *IET Renew. Power Gener.* **2017**, *11*, 1688–1694. [CrossRef]

159. Papaioannou, I.; Bouhouras, A.; Marinopoulos, A.; Alexiadis, M.; Demoulias, C.; Labridis, D. Harmonic impact of small photovoltaic systems connected to the LV distribution network. In Proceedings of the 2008 5th International Conference on the European Electricity Market, Lisbon, Portugal, 28–30 May 2008; pp. 1–6. [CrossRef]
160. Urbanetz, J.; Braun, P.; Rüther, R. Power quality analysis of grid-connected solar photovoltaic generators in brazil. *Energy Convers. Manag.* **2012**, *64*, 8–14. [CrossRef]
161. Klaić, Z.; Knežević, G.; Primorac, M.; Topić, D. Impact of photovoltaic and biogas power plant on harmonics in distribution network. *IET Renew. Power Gener.* **2020**, *14*, 110–117. [CrossRef]
162. Ahmed, A.; Iqbal, A.; Khan, I.; Al-Wahedi, A.; Mehrjerdi, H.; Rahman, S. Impact of EV charging station penetration on harmonic distortion level in utility distribution network: A case study of Qatar. In Proceedings of the IEEE Texas Power and Energy Conference (TPEC), Online, 2–5 February 2021; pp. 1–6. [CrossRef]
163. Staats, P.; Grady, W.; Arapostathis, A.; Thallam, R. A statistical analysis of the effect of electric vehicle battery charging on distribution system harmonic voltages. *IEEE Trans. Power Deliv.* **1998**, *13*, 640–646. [CrossRef]
164. Wanik, M. Harmonic measurement and analysis during electric vehicle charging. *Engineering* **2013**, *5*, 215–220. [CrossRef]
165. Wang, L.; Qin, Z.; Larumbe, L.; Bauer, P. Python supervised co-simulation for a day-long harmonic evaluation of EV charging. *Chin. J. Electr. Eng.* **2021**, *7*, 15–24. [CrossRef]
166. Slangen, T.M.H.; Cuk, V.; Cobben, J.F.G.; de Jong, E.C.W. Harmonic emission of EV fast charging station under different supply- and operating conditions. In Proceedings of the IEEE PES Innovative Smart Grid Technologies Conference Europe (ISGT Europe), Novi Sad, Serbia, 10–12 October 2022; pp. 1–5. [CrossRef]
167. *IEEE Std 1547a-2020 (Amendment to IEEE Std 1547-2018)*; IEEE Standard for Interconnection and Interoperability of Distributed Energy Resources with Associated Electric Power Systems Interfaces—Amendment 1: To Provide More Flexibility for Adoption of Abnormal Operating Performance Category III. Institute of Electrical and Electronics Engineers: New York, NY, USA, 2020. [CrossRef]
168. Li, R.; Zhu, J.; Hong, Q.; Booth, C.; Dysko, A.; Roscoe, A.; Urdal, H. Impact of low (zero) carbon power systems on power system protection: A new evaluation approach based on a flexible modelling and hardware testing platform. *IET Renew. Power Gener.* **2020**, *14*, 906–913. [CrossRef]
169. Miret, J.; Castilla, M.; Camacho, A.; de Vicuña, L.; Matas, J. Control scheme for photovoltaic three-phase inverters to minimize peak currents during unbalanced grid-voltage sags. *IEEE Trans. Power Electron.* **2012**, *27*, 4262–4271. [CrossRef]
170. Wang, F.; Duarte, J.; Hendrix, M. Pliant active and reactive power control for grid-interactive converters under unbalanced voltage dips. *IEEE Trans. Power Electron.* **2011**, *26*, 1511–1521. [CrossRef]
171. Tafti, H.D.; Maswood, A.I.; Pou, J.; Konstantinou, G.; Agelidis, V.G. An algorithm for reduction of extracted power from photovoltaic strings in grid-tied photovoltaic power plants during voltage sags. In Proceedings of the IEEE Industrial Electronics Society Annual Conference (IECON), Florence, Italy, 24–27 October 2016; pp. 3018–3023. [CrossRef]
172. Tafti, H.D.; Maswood, A.I.; Konstantinou, G.; Pou, J.; Acuna, P. Active/reactive power control of photovoltaic grid-tied inverters with peak current limitation and zero active power oscillation during unbalanced voltage sags. *IET Power Electron.* **2018**, *11*, 1066–1073. [CrossRef]
173. Miret, J.; Camacho, A.; Castilla, M.; de Vicuna, L.; Matas, J. Control scheme with voltage support capability for distributed generation inverters under voltage sags. *IEEE Trans. Power Electron.* **2013**, *28*, 5252–5262. [CrossRef]
174. Wang, J.; Wang, Y.; Zhong, Z.; Ma, G. Research on Prosumer Combining Household Electricity, Electric Vehicle Home Charging and Photovoltaic Power Generation. *Am. J. Electr. Electron. Eng.* **2019**, *7*, 18–23. [CrossRef]
175. Li, H.; Li, H.; Lu, W.; Wang, Z.; Bian, J. Optimal Power Flow Calculation Considering Large-Scale Photovoltaic Generation Correlation. *Front. Energy Res.* **2020**, *8*, 590418. [CrossRef]
176. Yu, H.; Huang, L.; Zhang, S.; Chen, H.; Tang, C.; Huang, Y. Effects of Distributed Photovoltaic Generation and Electric Vehicle Integrating into Distribution Network on Line Loss and Voltage Drift. *Smart Power* **2020**, *48*, 28–34.
177. Fu, J.; Han, Y.; Li, W.; Feng, Y.J.; Zalhaf, A.S.; Zhou, S.; Yang, P.; Wang, C.L. A novel optimization strategy for line loss reduction in distribution networks with large penetration of distributed generation. *Int. J. Electr. Power Energy Syst.* **2023**, *150*, 109112. [CrossRef]
178. Mahmud, K.; Hossain, M.; Ravishankar, J. Peak-load management in commercial systems with electric vehicles. *IEEE Syst. J.* **2019**, *13*, 1872–1882. [CrossRef]
179. Zhao, J.; Kucuksari, S.; Mazhari, E.; Son, Y.J. Integrated Analysis of High-Penetration PV and PHEV With Energy Storage and Demand Response. *Appl. Energy* **2013**, *112*, 35–51. [CrossRef]
180. Bajaj, M.; Singh, A.; Alowaidi, M.; Sharma, N.; Sharma, S.; Mishra, S. Power Quality Assessment of Distorted Distribution Networks Incorporating Renewable Distributed Generation Systems Based on the Analytic Hierarchy Process. *IEEE Access* **2020**, *8*, 145713–145737. [CrossRef]
181. Elbasuony, G.; Abdel Aleem, S.; Ibrahim, A.; Sharaf, A. A Unified Index for Power Quality Evaluation in Distributed Generation Systems. *Energy* **2018**, *149*, 607–622. [CrossRef]

182. Hu, Q.; Bu, S.; Terzija, V. A distributed p and q provision-based voltage regulation scheme by incentivized EV fleet charging for resistive distribution networks. *IEEE Trans. Transp. Electrif.* **2021**, *7*, 2376–2389. [CrossRef]
183. Wang, Y.; Qiu, D.; Strbac, G.; Gao, Z. Coordinated Electric Vehicle Active and Reactive Power Control for Active Distribution Networks. *IEEE Trans. Ind. Inform.* **2023**, *19*, 1611–1622. [CrossRef]
184. Gado, D.M.; Abou El-Ela, A.A.; Moussa, S.A. Power quality improvement for electric vehicle using hybrid active power filter. In Proceedings of the International Conference on Electrical Engineering and Energy Management (ICEEM), Menouf, Egypt, 3–4 July 2021; pp. 1–7. [CrossRef]
185. Qiu, D.; Wang, Y.; Hua, W.; Strbac, G. Reinforcement learning for electric vehicle applications in power systems: A critical review. *Renew. Sustain. Energy Rev.* **2023**, *173*, 113052. [CrossRef]
186. Wu, H.; Xu, Z. Prototype Federated Reinforcement Learning for Voltage Regulation in Distribution Systems With Physics-Aware Spatial-Temporal Graph Perception. *IEEE Trans. Sustain. Energy* **2026**, *17*, 697–708. [CrossRef]
187. Yan, T.; Dou, C.; Yue, D.; He, Z.; Li, H. Rapid Active Power Regulation of Distributed Photovoltaics Based on Optimal Dynamic Droop Coefficients. *IEEE Trans. Sustain. Energy* **2026**, *17*, 158–170. [CrossRef]
188. Coppez, G.; Chowdhury, S.; Chowdhury, S. Impacts of energy storage in distributed power generation: A review. In Proceedings of the International Conference on Power System Technology, , Zhejiang, China, 24–28 October 2010; pp. 1–7. [CrossRef]
189. Jing, W.; Lai, C.H.; Wong, W.S.; Wong, M.D. A comprehensive study of battery-supercapacitor hybrid energy storage system for standalone PV power system in rural electrification. *Appl. Energy* **2018**, *224*, 340–356. [CrossRef]
190. Zhang, L.; Hu, X.; Wang, Z.; Sun, F.; Deng, J.; Dorrell, D.G. Multiobjective optimal sizing of hybrid energy storage system for electric vehicles. *IEEE Trans. Veh. Technol.* **2018**, *67*, 1027–1035. [CrossRef]
191. Hu, L.; Tian, Q.; Zou, C.; Huang, J.; Ye, Y.; Wu, X. A study on energy distribution strategy of electric vehicle hybrid energy storage system considering driving style based on real urban driving data. *Renew. Sustain. Energy Rev.* **2022**, *162*, 112416. [CrossRef]
192. Wu, X.; Hu, X.; Yin, X.; Moura, S.J. Stochastic optimal energy management of smart home with pev energy storage. *IEEE Trans. Smart Grid* **2018**, *9*, 2065–2075. [CrossRef]
193. Song, T.; Wang, P.; Zhang, Y.; Gao, F.; Tang, Y.; Pholboon, S. Suppression method of current harmonic for three-phase PWM rectifier in EV charging system. *IEEE Trans. Veh. Technol.* **2020**, *69*, 9634–9642. [CrossRef]
194. Balasundar, C.; Sundarabalan, C.; Sharma, J.; Srinath, N.; Guerrero, J. Design of power quality enhanced sustainable bidirectional electric vehicle charging station in distribution grid. *Sustain. Cities Soc.* **2021**, *74*, 103242. [CrossRef]
195. Chen, F.; Ruijie, L.; Guanhua, L. Research on harmonic analysis and harmonic suppression measures of electric vehicle charging station. In Proceedings of the IEEE International Conference on Advances in Utility Research and Electrical Engineering (AUTEEE), Shenyang, China, 22–24 November 2019; pp. 71–75. [CrossRef]
196. Zhou, N.; Wang, J.; Wang, Q.; Wei, N. Measurement-based harmonic modeling of an electric vehicle charging station using a three-phase uncontrolled rectifier. *IEEE Trans. Smart Grid* **2015**, *6*, 1332–1340. [CrossRef]
197. Bai, S.; Lukic, S. Unified active filter and energy storage system for an mw electric vehicle charging station. *IEEE Trans. Power Electron.* **2013**, *28*, 5793–5803. [CrossRef]
198. Vasiladiotis, M.; Rufer, A. A modular multiport power electronic transformer with integrated split battery energy storage for versatile ultrafast EV charging stations. *IEEE Trans. Ind. Electron.* **2015**, *62*, 3213–3222. [CrossRef]
199. Rao, P.; Crow, M.; Yang, Z. STATCOM control for power system voltage control applications. *IEEE Trans. Power Deliv.* **2000**, *15*, 1311–1317. [CrossRef]
200. Moghbel, M.; Masoum, M.A.S. D-STATCOM based on hysteresis current control to improve voltage profile of distribution systems with PV solar power. In Proceedings of the Australasian Universities Power Engineering Conference (AUPEC), Brisbane, Australia, 25–28 September 2016; pp. 1–5. [CrossRef]
201. Harish, B.; Surendra, U. Power quality disturbance mitigation in grid connected photovoltaic distributed generation with plug-in hybrid electric vehicle. *Int. J. Electr. Comput. Eng. (IJECE)* **2023**, *13*, 6025–6036. [CrossRef]
202. Balasundar, C.; Sundarabalan, C.; Santhanam, S.; Sharma, J.; Guerrero, J. Mixed step size normalized least mean fourth algorithm of DSTATCOM integrated electric vehicle charging station. *IEEE Trans. Ind. Inform.* **2023**, *19*, 7583–7591. [CrossRef]
203. *IEEE Std 1547.9-2022*; IEEE Guide for Using IEEE Std 1547 for Interconnection of Energy Storage Distributed Energy Resources with Electric Power Systems. Institute of Electrical and Electronics Engineers: New York, NY, USA, 2022. [CrossRef]
204. *EN 50549-1:2019+A1:2023*; Requirements for Generating Plants to Be Connected in Parallel with Distribution Networks—Part 1: Connection to a LV Distribution Network—Generating Plants up to and Including Type B. European Committee for Electrotechnical Standardization: Brussels, Belgium, 2023.
205. *EN 50549-2:2019+A1:2023*; Requirements for Generating Plants to Be Connected in Parallel with Distribution Networks—Part 2: Connection to a MV Distribution Network—Generating Plants up to and Including Type B. European Committee for Electrotechnical Standardization: Brussels, Belgium, 2023.

206. *IEC TR 61000-3-6:2008*; Electromagnetic Compatibility (EMC)—Part 3-6: Limits—Assessment of Emission Limits for the Connection of Distorting Installations to MV, HV and EHV Power Systems. International Electrotechnical Commission: Geneva, Switzerland, 2008.
207. *IEC TR 61000-3-14:2011*; Electromagnetic Compatibility (EMC)—Part 3-14: Assessment of Emission Limits for Harmonics, Interharmonics, Voltage Fluctuations and Unbalance for the Connection of Disturbing Installations to LV Power Systems. International Electrotechnical Commission: Geneva, Switzerland, 2011.
208. *IEC TR 61000-3-15:2011*; Electromagnetic Compatibility (EMC)—Part 3-15: Limits—Assessment of Low Frequency Electromagnetic Immunity and Emission Requirements for Dispersed Generation Systems in LV Network. International Electrotechnical Commission: Geneva, Switzerland, 2011.
209. International Electrotechnical Commission. *Secondary Cells and Batteries Containing Alkaline or Other Non-Acid Electrolytes—Safety Requirements for Secondary Lithium Cells and Batteries, for Use in Industrial Applications*; International Electrotechnical Commission: Geneva, Switzerland, 2022.
210. International Organization for Standardization. *Road Vehicles—Vehicle to Grid Communication Interface—Part 20: 2nd Generation Network Layer and Application Layer Requirements*; International Organization for Standardization: Geneva, Switzerland, 2022.
211. International Organization for Standardization. *Road Vehicles—Vehicle to Grid Communication Interface—Part 20: 2nd Generation Network Layer and Application Layer Requirements— Amendment 1: AC DER Service, MCS Service, and Improved Security Concept*; International Organization for Standardization: Geneva, Switzerland, 2026.
212. Institute of Electrical and Electronics Engineers. *IEEE Standard Conformance Test Procedures for Equipment Interconnecting Distributed Energy Resources with Electric Power Systems and Associated Interfaces*; Institute of Electrical and Electronics Engineers: New York, NY, USA, 2020.
213. *IEC 61000-3-2:2018+AMD1:2020+AMD2:2024 CSV*; Electromagnetic Compatibility (EMC)—Part 3-2: Limits—Limits for Harmonic Current Emissions (Equipment Input Current ≤ 16 A per Phase). Consolidated Version, Edition 5.2. International Electrotechnical Commission: Geneva, Switzerland, 2024.
214. *IEC 61000-3-12:2011+AMD1:2021 CSV*; Electromagnetic Compatibility (EMC)—Part 3-12: Limits—Limits for Harmonic Currents Produced by Equipment Connected to Public Low-Voltage Systems with Input Current > 16 A and ≤ 75 A per Phase. Consolidated version, Edition 2.1; International Electrotechnical Commission: Geneva, Switzerland, 2021.
215. *IEC 61000-2-2:2002+AMD1:2017+AMD2:2018 CSV*; Electromagnetic Compatibility (EMC)—Part 2-2: Environment—Compatibility Levels for Low-Frequency Conducted Disturbances and Signalling in Public Low-Voltage Power Supply Systems. Consolidated Version, Edition 2.2. International Electrotechnical Commission: Geneva, Switzerland, 2018.
216. *IEC 61000-2-12*; Electromagnetic Compatibility (EMC)—Part 2-12: Environment—Compatibility Levels for Low-Frequency Conducted Disturbances and Signalling in Public Medium-Voltage Power Supply Systems. International Electrotechnical Commission: Geneva, Switzerland, 2003.
217. Nduka, O.; Kunjumuhammed, L.; Pal, B.; Majumdar, A.; Yu, Y.; Maiti, S.; Ahmadi, A. Field Trial of Coordinated Control of PV and Energy Storage Units and Analysis of Power Quality Measurements. *IEEE Access* **2019**, *8*, 1962–1974. [CrossRef]
218. Xin, T.; Fan, S.; Chang, P.; Yang, Q.; Bao, Y.; Zhang, W.; Liu, P. Day-Ahead Optimal Scheduling for Electric Bus PV-Storage Charging Station Under Uncertainty: An IGDT-Based Approach. *Batteries* **2026**, *12*, 167. [CrossRef]
219. Li, C.; Carta, D.; De Din, E.; Benigni, A. MPC-Based Multifunctional V2G Operation in Multienergy Systems. *IEEE Open J. Ind. Electron. Soc.* **2026**, *7*, 28–41. [CrossRef]

Disclaimer/Publisher's Note: The statements, opinions and data contained in all publications are solely those of the individual author(s) and contributor(s) and not of MDPI and/or the editor(s). MDPI and/or the editor(s) disclaim responsibility for any injury to people or property resulting from any ideas, methods, instructions or products referred to in the content.